

IUGG General Assembly, Vienna, August 1991
Union Lecture

**TIDAL INTERACTIONS
IN THE EARTH MOON SYSTEM**

Paul Melchior

Observatoire Royal de Belgique
Bruxelles

Freely-available file downloaded from
<http://www.agu.org/books/sp/v035/SP035p0047/SP035p0047.pdf>

1 History

Tides are a planetary phenomenon. It affects the whole body of the Earth from its centre to its surface, the oceans and the underground waters, creating deformations and stresses which perturb all kinds of precise measurements.

To my knowledge the tides are the only geophysical phenomenon where we a priori know, with a very high precision, the forces in action. The reciprocal masses of Earth Moon and Sun are known indeed with a precision of 2.10^{-6} while the frequencies in the orbital motions and their perturbations as well as the frequency of the rotation of the Earth are known with 7 digits exact.

Tides on the Earth is a differential phenomenon as it results from the difference of the applied forces between a point on or inside the Earth and the applied forces at its Centre of Mass. It is thus a global planetary phenomenon of very long wavelength and, consequently it will be difficult to extract local or even regional informations. However tidal phenomena concern a frequency band (periods from 8 hours to 30 hours) which is between the seismic and free oscillations frequencies (periods less than 1 hour) and the polar motion period (434 days). This makes them specially important.

The history of the man approach to the understanding of tidal phenomena apparently starts with the campaigns of Alexander the Great and of Caius Julius Caesar when their mediterranean soldiers reached the shores of the Indian Ocean and of the Atlantic Ocean: astonishment and, even, terror in front of semi-diurnal high oceanic tides are reported and already related to the Moon in famous texts of the Antiquity (Figure 1).

More unexpected for us is the first observation of an earth tide effect by Strabon (+25 J.C.) in the form of an inverted tide [*αντιπαθειν*] in water wells submitted to alternative cubical dilatations and compressions by the crustal tides (Figure 2).

I propose to consider in this one hour talk three epochs in the development of our knowledge of tidal interactions:

7. Φησὶ δὲ ὁ Πολύβιος κρήνην ἐν τῷ Ἡρακλείῳ τῷ ἐν Γαδείροις εἶναι, βαθμῶν ὀλίγων κατὰβασιν ἔχουσιν εἰς τὸ ὕδωρ πότιμον, ἣν ταῖς παλιρροίαις τῆς θαλάττης
 → ἀντιπαθεῖν, κατὰ μὲν τὰς πλήμας ἐκλείπουσαν, κατὰ δὲ τὰς ἀμπώτεις πληρουμένην.

Figure 1: Strabon, Geography L.III (+25 J.C.) referring to Polybius (205-123 before J.C.) from original source Silanos (III-II century before J.C.)

Eadem nocte accidit, ut esset luna plena, qui dies maritimos aestus maximos in Oceano efficere consuevit, nostrisque id erat incognitum. ita uno tempore et longas naves, quibus Caesar exercitum transportandum curaverat quasque in aridum subduxerat, aestus complebat, et onerarias, quae ad ancoras erant deligatae, tempestas adfliebat, neque ulla nostris facultas aut administrandi aut auxiliandi dabatur. compluribus navibus fractis reliquae cum essent funibus, ancoris reliquisque armamentis amissis ad navigandum inutiles, magna, id quod necesse erat accidere, totius exercitus perturbatio facta est.

Figure 2: C.IVLII Caesaris Commentarii Rerum Gestarum. Vol I - Bellum Gallicum

- the epoch of pioneers from Newton to the International Geophysical Year "IGY1957"
- a transition period from IGY1957 up to 1980 when we did not have the powerful tools that we have today, but already had improved quartz clinometers, recording gravimeters and the first "electronic computer" (the glorious IBM650)
- the present days with powerful computers, VLBI, superconducting gravimeters (1982), excellent models of the earth's internal structure and quite good models of the oceanic tides (1979).

Newton, in his Principiae, used the observed ratio between lunar and solar principal oceanic tides to evaluate the respective contributions of Moon and Sun in the luni-solar precession of the earth's axis in space, pointing out, in this way, from the very beginning, the same gravitational origin of tides and precession-nutations (1687).

Kant, in 1754, argued that a secular retardation of the earth's speed of rotation must be a consequence of tidal friction.

The first essential contribution to the understanding of most of the peculiarities of tidal phenomena is certainly due to Laplace in 1799 who identified the three species of second order tides by a simple trigonometric treatment and the use of Legendre polynomials (Figure 3):

- a semi-diurnal family of tides with a geographical distribution represented by a sectorial spherical harmonic function ($n=m$ in eqn.1)
- a diurnal family with a distribution represented by a tesseral spherical harmonic function ($m < n$ in eqn.1)
- a fortnightly monthly, semi-annual and annual family with a distribution represented by a zonal spherical harmonic function ($m=0$ in eqn.1).

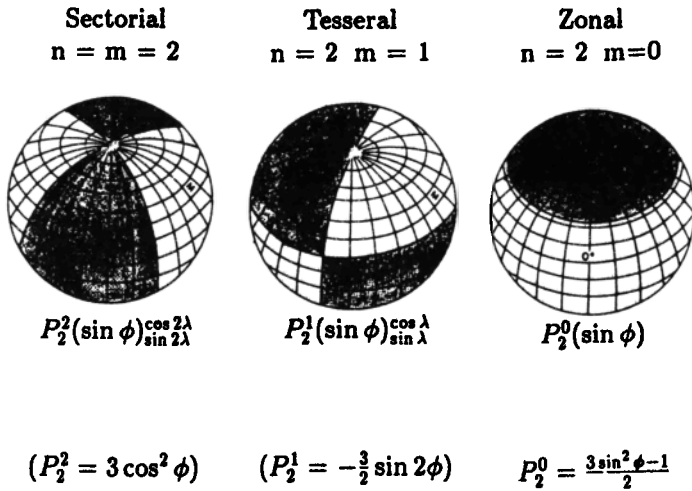


Figure 3: The three families of tides (Laplace)

The sectorial family would be responsible for a secular retardation of the earth's rotation speed due to friction.

The tesseral family is associated with precession and nutations. The zonal family provokes periodic fluctuations of the earth's rotation speed.

The general expression of the tidal potential can be written as follows:

$$W = \sum_{n=2}^{\infty} \sum_{m=0}^n K_n \sum_i A_{nmi} \cos[\omega_i t + \frac{1}{2}(n-m)\pi] P_n^m(\sin \phi) \quad (1)$$

In 1876 Lord Kelvin developed a great deal of mathematical analysis of the elastic deformations of a homogeneous incompressible elastic sphere of radius r , density ρ and superficial gravity g submitted to an external gravitational potential W_2 of order 2 and obtained the famous formula which relates the periodic radial deformation $h \frac{W_2}{g}$ due to this external potential to the rigidity μ of an homogeneous spherical, non rotating and oceanless earth:

$$h \frac{W_2}{g} = \frac{5}{2} \left[1 + \frac{19\mu}{2g\rho a} \right]^{-1} \frac{W_2}{g} \quad (2)$$

with

$$kW_2 = \frac{3}{2} \left[1 + \frac{19\mu}{2g\rho a} \right]^{-1} W_2, \quad k = \frac{3}{5} h \quad (3)$$

the h and k dimensionless numbers are transfer functions which characterize the radial deformation and the variation of the gravitational potential due to the tidal deformation. This formula was used by G. Darwin in 1882 to derive the mean rigidity of the Earth from the reduction of oceanic tidal amplitude by the Earth crust tidal amplitude h (which reaches some 40 centimeters).

With an observed value of $1 + k - h = 0.68$, he deduced that the earth's mean rigidity was that of steel. On the other hand, since 1879 Darwin had already developed a number of fundamental papers on tidal theory and tidal analysis.

It was already during the last century that mathematicians became concerned with the problems deriving from the existence of an ellipsoidal non viscous liquid core rotating inside a rigid thick shell (Hough 1895, Sludsky, 1895) which culminated with an illuminating paper of Poincaré in 1910. The problem of the liquid core was revisited by Jeffreys in 1948 and later became one of our major concerns in tidal research since IGY 1957 when Molodensky (1961) published a new theoretical approach which was soon experimentally verified. A fundamental step was achieved by A.E.H. Love in 1911 who introduced the concept of parameters specific to spherical elasticity which are universally used and called the "Love numbers": h, k, ℓ (as used in the previous equation (2) and (3)).

This concept of transfer function has been extended to an uniformly rotating slightly elliptical Earth with an elastic inner core, a liquid outer core and an elastic mantle by J. Wahr (1981) who introduced latitude dependent Love numbers.

Later on, the effect of mantle inelasticity has been fully incorporated in the equations by Dehant (1987) who used complex shear modulus profiles and derived complex differential equations which, integrated, yield complex tidal parameters.

If the orbits of the Earth and Moon were perfectly circular, if the ecliptic and orbital plane of the Moon were in the earth equatorial plane, then the number of tidal components would be restricted to only two: one lunar and one solar semi diurnal waves. The inclination of the orbital planes upon the equator, the ellipticities of the two orbits, the evection and variation which are perturbations of the ellipticity of the Moon's orbit by the Sun and every kind of perturbation produce splittings of the fundamental spectral lines and the generation of an infinity of tidal components. It is thus necessary to truncate the development at a level which corresponds to the precision of the instruments in use at every epoch.

In 1883 Darwin published the first harmonic development of the tidal potential with no more than 39 terms which was surely compatible with the precision of tidal gauges and tiltmeters in the last century. It was in 1921 that Doodson gave an extended development up to 386 waves. This was improved and extended to 505 waves in 1973 by Cartwright Tayler and Edden. Since 1985 several new developments have been published containing up to 1200 waves. Some waves even result from the perturbations of the planets Venus and Jupiter on the Earth's orbit (Tables I, II). This is now necessary in view of the interpretation of tidal measurements performed with superconducting gravimeters.

2 Analysis

As mentioned before, thanks to centuries of Fundamental Astronomy observations, we know all the tidal frequencies with a 7 digit accuracy, a precision that no spectral analysis can obtain.

Table I. Number of terms in the Tidal Development

	Digits on <i>A_{nmi}</i>	Long Period	Diurnal	Semi Diurnal	Ter Diurnal	Fourth Diurnal	Total	σ
Doodson (1921	5	99	158	115	14	-	386	50
Cartwright-Tayler	5	128	205	155	17	-	505	
Edden (1973)								
Bullesfeld (1985)	5	169	246	195	42	4	656	35
Xi Qin Wen (1987)	5	263	457	374	77	7	1178	40
Tamura (1987)	6(+)	281	450	377	82	10	1200	15
(*)		2	2	4				

σ : standard deviation in nanogals according to the analysis of a theoretical series (Wenzel)
(*) : numbers of included terms from Venus and Jupiter
(+) : corresponds to 0.8 nanogal for each constituent

Table II. Limits of the Tidal frequency bands (ω : degrees per hour) and periods (P : hours)




Author		Long Period	Diurnals		Semi Diurnals	
						
Doodson (1922)	ω	3.20268	11.76554	17.69937	26.33508	31.72675
	P	112.406	30.598	20.340	13.670	11.347
Cartwright-Tayler Edden (1971)	ω	3.20268	11.76554	17.69937	26.33508	31.72675
	P	112.406	30.598	20.340	13.670	11.347
Bullesfeld (1985)	ω	3.27553	11.29402	17.77223	26.33508	32.26892
	P	109.906	31.875	20.256	13.670	11.156
Xi Qinwen (1987)	ω	3.67420	11.29402	17.77443	26.33508	32.27113
	P	97.981	31.875	20.254	13.670	11.155
Tamura (1987)	ω	3.74926	10.82249	18.24595	25.79071	32.74265
	P	96.019	33.264	19.730	13.959	10.995

Table III. Main Tidal waves usually separated by harmonic analysis.

Darwin Symbol	Number of Sideband Constituents	Period in hours	Amplitude Coefficient A_{nmi}	Origin	
Tesseral diurnal declinational					
Q1	32	26.858	7216	lunar	elliptic of O1
O1	31	25.819	37689	lunar	principal
P1	9	24.066	17554	solar	principal
K1	17	23.934	53050	luni-solar	sidereal
ψ 1	3	23.869	423	solar	elliptic of K1
J1	19	23.098	2964	lunar	elliptic of K1
Sectorial Semi diurnal					
μ 2	20	12.872	2777	lunar	variation
N2	24	12.658	17387	lunar	elliptic
ν 2	24	12.626	3303	lunar	evection
M2	55	12.421	90812	lunar	principal
λ 2	12	12.222	670	lunar	evection
L2	25	12.192	2567	lunar	elliptic
S2	6	12.000	42286	solar	principal
K2	27	11.967	11506	luni-solar	declinational
Sectorial Ter diurnal					
M3	45	8.280	1180	lunar	principal
Zonal Long Period					
Mf	5	13.661	15642	lunar	declinational

one vertical bar: six months observation are needed to separate these components

two vertical bars: one year observation is needed to separate these components

As a result, considering these frequencies as known, the tidal "harmonic" analysis procedure introduced by Kelvin in 1868 is now performed by least squares, which uses specially designed numerical filters to separate the three Laplace species of tides before extracting as many spectral lines as possible in relation to the length of the record. Actually, each "line" is a tidal band containing many minor sideband components which are very close in frequency and are supposed to have the same response as the main "line" of their band (Table III).

When the response of the earth in amplitude and phase has been experimentally obtained in this way, given a number of tidal frequencies, it becomes easy to subtract a reconstructed tidal effect based upon this experimental response from the original data set to obtain a time series of residues which can then be analyzed by spectral methods to search for possible non

tidal spectral lines For a long time, non-tidal lines were never found. It is a controversial result whether such lines recently found in the records of a superconducting gravimeter are real or not.

Other procedures are of course developed like the "response method", multiple linear regression analysis, Bayesian statistical modeling, with the aim to take into account the effects of environmental data, principally atmospheric pressure and, to a lesser extent, temperature fluctuations.

3 Instruments

To observe such minute variations of the gravity vector necessitates obviously ingenious instruments, but during the last century, when electronics were inexistent, the invention of the horizontal pendulum by Lorenz Hengler in 1832 and subsequent slow developments enabled Von Rebeur Paschwitz to register, on photographic paper, the tidal oscillations of the direction of the vertical. These measurements were made at various locations in Germany and in the Canarias Islands (1891-92).

Before the years 1950, no gravimeter was sufficiently accurate to obtain a precision better than one half of a milligal. All observations were restricted to tilt measurements with such horizontal pendulums. However, Michelson himself succeeded to observe them in a 150 meters long water tube by evidently applying his famous expertise in interferometry (1914).

Most of these tilt measurements were performed in Germany and as soon as 1907 Hecker noted a systematic difference between the observed response in North South and in East West directions. He attributed them to indirect effects due to ocean-continent tidal interactions in form of attraction of the sea waters upon the pendulum's beam and flexure of the crust under the variable loading effect of the same sea waters. A third effect results from a change of the gravitational potential of the deformed upper mantle under this load.

Nevertheless, measurements of variations of the order of $0''04$ were still considered mere curiosity without practical applications in Geodesy as levellings and triangulations could not be performed with such precisions.

At a time when Seismology was still in its infancy, however, the results of these periodic tilt measurements allowed Kelvin (1863) to refute the model of an earth with a thin crust and a completely fluid interior. Later on, Jeffreys used them to investigate the elastic properties of an earth model with a thick mantle and a liquid core. Finally, still before the IGY 1957 year, Takeuchi (1950) using numerical methods to solve the differential equations for a realistic earth model, established an upper limit ($\mu < 10^{10}$ dyne cm^{-2} or 10^9 Pa - two orders of magnitude less than the Lower Mantle where μ is of the order of $3 \cdot 10^{11}$ Pa) for the rigidity of the core on the basis of these preliminary measurements.

Table IV. Number of publications about Earth Tides

1800 - 1900	72	1961 - 1965	433
1901 - 1920	64	1966 - 1970	485
1921 - 1940	161	1971 - 1975	678
1941 - 1956	213	1976 - 1980	796
1957 - 1960	260	1981 - 1985	578
		1986 - 1989	(579)

Since 1980 the subject became so broad that it is often difficult to decide if a paper belongs to the earth tides subject only or to oceanography, physics of the earth interior, space geodesy, hydrology...

The numbers reported here concern only earth tides but it is often a matter of appreciation.

Since the Madrid General Assembly in 1924, the International Association of Geodesy had established as a rule to have every three years a "Rapport sur les Marées de l'Ecorce Terrestre" which was established by Walter Lambert from 1924 to 1954 where all papers published on the subject were exhaustively reported and analyzed. When I succeeded Walter Lambert in this task in 1957, it soon became impossible to make such reports because of the rapidly increasing number of papers on the subject. As in most geodetic and geophysical fields, IGY 1957 was the great impulse for our finishing century and IAG immediately established a Permanent Commission on Earth Tides and a Center in charge of computations and data collection. Not only were new instrumentation involving electronics being developed but the first electronic computer IBM 650 became available and allowed for the first time to make calculations -albeit slow, which were not possible with desk mechanical machines.

Table V. Core Resonance
Tilt amplitude factor $\gamma = 1 + k - h$

Theoretical Amplitude at 50° Latitude		Observed			Theoretical results	
Wave		Sclaigneaux (1960)	Dourbes (1966)	Jeffreys (1950)	Molodensky (1961)	Wahr-Dehant (1987)
O1	0°00478	0.696	0.666	0.658	0.686	0.695
P1	0°00222	0.722	0.704	0.676	0.697	0.705
K1	0°00672	0.757	0.757	0.714	0.726	0.736

Depth: Sclaigneaux 85m, Dourbes 46m

Tiltmeters measure the combination $1 + k - h$ of the Love numbers. They were considerably improved by the use of very thin suspension wires made of quartz, reaching a really high sensitivity of the order of 0°0001. They were calibrated with an accuracy of 0.5% with dilatable bearing plates invented by Verbaandert (1960). It is with such simple instruments that the core resonance on the diurnal tidal waves predicted and evaluated by Jeffreys in 1950 was experimentally firmly established in 1966 in two different underground deep stations Sclaigneaux and Dourbes in Belgium (Table V).

But, because it was later realized that there must be a coupling between strain and tilt strongly dependent upon the complicate local conditions in the underground mine galleries or rooms, the tiltmeters lost much favor in the determination of the elastic earth response to tides. Some hope to overcome these difficulties may come with the use of borehole tiltmeters.

Nevertheless they had allowed to measure experimentally the core resonant effects because the strain-tilt coupling is similar on frequencies sufficiently close as those of the diurnal waves. Unfortunately the noise level in tilt measurements does not permit to go further in the comparison with different earth core stratification models.

Gravimeters measure the combination $\delta = 1 + h - \frac{3}{2} k$ of the Love numbers. The first automatically recording spring gravimeters were constructed between 1954 and 1957 by Lecolazet in Strasbourg and by Brein in Frankfurt who adapted photographic systems on rebuilt North American gravimeters.

At the same epoch the LaCoste Romberg astaticized gravimeters became available in many places as well as static Askania gravimeters but after some 10 years the static instruments were progressively abandoned in favour of the more sensitive astaticized ones which, since 1980, were progressively equipped with feedback systems. Such instruments allow to achieve a precision of about 0.3 microgal ($3 \cdot 10^{-10}$ of g) in the determination of the amplitudes of the tidal waves. However the problem of calibration of these spring gravimeters remains critical even if an accuracy of 0.5% in the very small range of observed variations seems to be reached now.

Indirect methods are used for their calibration: measurements on baselines, comparisons between many instruments while the only direct determination achieved with success is obtained on a platform oscillating at some 10 different frequencies with a one centimetre amplitude.

A most important development is obviously the construction in California of the first cryogenic gravimeter (1971) which, using the superconductive properties of a small ball maintained in levitation in a perfectly stable magnetic field within a liquid helium bath, allows to speak now in terms of nanogals, that is 10^{-12} of g.

The initial objective of those few observatories which installed such instruments was to obtain the best possible determination of the resonant response on diurnal frequencies. The first two stations established in Europe at Bruxelles and Bad Homburg (Germany) have given in this respect a new view on the subject in full agreement with VLBI nutations measurements as we will see later (Neuberg et al. 1987, §9).

Of course, as it is always the case, new objectives are now assigned to a worldnet of superconducting gravimeters. These objectives are submitted here to a discussion by SEDI.

It must be pointed out again that the calibration in amplitude and marginally in phase is still a problem with this kind of instrument.

After some fifteen years from IGY 1957 it appeared that tidal gravity measurements had been performed only in Europe, North America and Japan so that a real need appeared for establishing what has been called "Trans World Tidal Gravity Profiles". With this programme, started in 1973, some 125 stations were established in Africa, Asia, Australia, New Zealand, South Pacific, Latin America and Caraïbes by the International Centre for Earth Tides (Brussels). The ICET Data Bank contains now 327 different stations. The UCLA South Pole station is to be mentioned specially here.

A main goal was to check if the modelling of the ocean-continent tidal interactions was possible and correct. As a matter of fact this operation established serious imperfections of the few available oceanic cotidal maps.

Only the M_2 tidal wave had been investigated in details even if one or two maps existed for K_1 , O_1 and S_2 (Bogdanov and Magarik).

The tentative comparisons between the observed gravity tides with these ocean models

were thus really disappointing until cotidal maps corresponding to eleven main tidal waves constructed by E. Schwiderski became available in 1979.

The linear deformations induced by the earth tides are rather easy to measure either with laser beam extensometers, or with mechanical extensometers (wires or bars) equipped with electronic transducer detectors. They clearly appear in VLBI measurements.

These deformations and the resulting cubic dilatations are however quite small, of the order of 10^{-8} of the length of the considered baseline. If the Lamé elastic constants are about 10^{11} Pascal, horizontal and vertical stresses of 1 to 6×10^3 Pascal result for the main tidal wave M2 which is more or less 1/1000 of the tectonic stresses measured in Western Europe. Nevertheless the tidal stresses, despite their small size, are often considered to be capable to trigger earthquakes in seismically active areas. Oceanic tidal loading creates only slightly bigger effects: $\sigma_{rr} = 20 \times 10^3$ Pa for a 2 meters oceanic tide amplitude.

4 Ocean Tides

Understanding and modelling the complicate features of the oceanic tides has been one of the most difficult challenges in geophysics. Even at one recent time there was some discouragement and people were ready to abandon the project (the International Working Group on oceanic Tides dissolved itself at our Grenoble General Assembly in 1975).

Though, we know, a priori, the frequency and the amplitude of each of the numerous components of the astronomical tide generating potential which should allow us to map each corresponding ocean tide, it was only ten years ago that a satisfactory solution was obtained for the first time.

The basic equations were already given by Laplace but several essential terms had to be added to obtain a realistic description of the phenomenon:

1. the friction at the bottom of the ocean
2. the viscous turbulent dissipation (the enormous dimensions of the world ocean make the Reynolds number extremely high)
3. a secondary tidal potential W' representing a combination of
 - the newtonian potential perturbation due to self gravitation of oceanic tides
 - the elastic potential perturbation due to the deformation of the ocean bottom under the oceanic tidal load (load number k'_n)
 - the actual deformations of the solid earth bottom by the oceanic load (load number h'_n) (Figure 4)

The method of evaluation of these important effects is originally due to Boussinesq (1878), improved by Longman (1962) by the use of Green's functions and fully developed by Farrell (1972). The calculation of the attraction is straightforward while the calculation of the elastic deformation due to the load has been made feasible when Munk and Mac Donald introduced in 1959 a new family of so called "Love loading numbers" h'_n k'_n which are negative dimensionless numbers (the load produces a depression only partly compensated by the loading mass attraction).

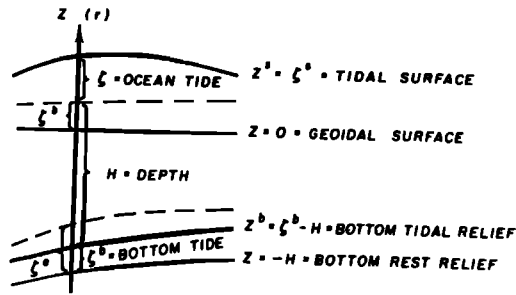


Figure 4:

Earth-ocean tidal interaction: ξ = ocean tide, ξ^s = earth tide, ξ^s = surface tide, ξ^b = bottom tide, $\xi^{so} = \xi^s - \xi^b$ = earth dip-response to ocean tide, and H = ocean depth. (Schwiderski 1980)

The load numbers must be calculated over a large range, typically from $n=0$ to $n=10.000$ but they have an asymptotic behaviour.

The secondary potential W' , proportional to $(1 + k'_n - h'_n)$ was introduced in the equations by Hendershott in 1972.

Including of course Coriolis and centrifugal forces, the equations of conservation of momentum and mass take the form

$$\begin{aligned} \frac{\partial u}{\partial t} - 2\omega v \cos \theta &= (1 + k - h) \frac{\partial W}{a \sin \theta \partial \lambda} + \frac{\partial W'}{a \sin \theta \partial \lambda} - g \frac{\partial \xi}{a \sin \theta \partial \lambda} - \nu \frac{\sqrt{u^2 + v^2}}{D} u + \nu^* \Delta_H u \\ \frac{\partial v}{\partial t} + 2\omega u \cos \theta &= (1 + k - h) \frac{\partial W}{a \partial \theta} + \frac{\partial W'}{a \partial \theta} - g \frac{\partial \xi}{a \partial \theta} - \nu \frac{\sqrt{u^2 + v^2}}{D} v + \nu^* \Delta_H v \\ \frac{\partial \xi}{\partial t} - \frac{\partial \zeta}{\partial t} + \frac{1}{a \sin \theta} \left[\frac{\partial}{\partial \lambda} (uD) + \frac{\partial}{\partial \theta} (vD \sin \theta) \right] &= 0 \\ \Delta_H &= \frac{\partial^2}{a^2 \sin^2 \theta \partial \lambda^2} + \frac{\partial^2}{a^2 \partial \theta^2} \end{aligned} \quad (4)$$

(u, v are the velocity components; $D = D(\theta, \lambda)$ is the depth of the ocean; ξ is the height of the oceanic free surface and ζ the height of the static tide W_2/g above the undisturbed surface).

Free slip and, possibly, no cross flow should be the prescribed boundary conditions along the continents shores. Sea surface elevations are prescribed by observations at some places. Moreover mass should be conserved in the Oceans but this is usually not perfectly satisfied.

As soon as electronic computers became available, many authors tried to numerically integrate these equations.

They had therefore to cover the oceanic areas with a grid ($1^\circ \times 1^\circ$ corresponding to some 45000 polygons), introduce the bathymetry (from 5 meters to 7000 meters) by adoption of a mean depth in each $1^\circ \times 1^\circ$ spherical trapezium, model the zigzagging geometric boundaries and make some hypothesis about friction and eddy viscosity.

in the most recent version, which presently looks the most satisfactory world map to external checks by altimetry, bottom pressure recorders in deep sea areas or loading in solid earth tides, Schwiderski preferred a linear law of bottom friction (with a friction coefficient $b = 0.01 \text{ m s}^{-1}$) and a lateral eddy viscosity ν^* proportional to the mean lateral cross-section area (thus to the depth $D : aD(1 + \sin \theta)/2$ which is found to be comprised between $1.3 \cdot 10^3$ and $1.3 \cdot 10^6 \text{ m}^2 \text{ s}^{-1}$) both being empirically adjusted by trial and error computations aiming to realize, by hydrodynamical interpolation, the best possible agreement with some 2000 tide gauge stations around the world.

Schwiderski shows how the introduction of viscosity is essential: it keeps the instability of the flow under control and permits to overcome the resonance threats at certain ocean depths.

The eddy dissipation is essentially effective in the deep ocean, while bottom friction is mainly significant in shallow seas.

The introduction of the secondary potential is also necessary even if it does not play such an essential role as viscosities but it makes some improvement in the solution.

On all cotidal maps, the tides are rotating around amphidromic (null amplitude) points due to the presence of the continents and to the Coriolis force which in principle makes them turn counterclockwise in the northern hemisphere and clockwise in the southern hemisphere (Figure 5a, 5b). There are some twenty M_2 and twelve O_1 amphidromic points in the open world ocean but there are many more in gulfs, straits and smaller areas (examples are the Adriatic Sea, the Corea sea, the Hudson Bay and many others). Schwiderski has constructed not less than eleven cotidal-corange maps for the main waves Ssa, Mm, Mf, Q1, O1, P1, K1, N2, M2, S2, K2. The accuracy he claims is 5 cm in amplitude for each partial tide and 10 cm for the combined tide. Controls by other authors do not really contradict this but it seems that some extreme discrepancies could reach 15 cm. Comparisons with deep sea pressure gauges are of course helpful to test the validity of cotidal maps. Addition of five smaller semi diurnal constituents $2N_2$, μ_2 , ν_2 , L_2 , T_2 from spline interpolation in the frequency domain (LeProvost et al. 1991) result in a significant improvement in accuracy of the Schwiderski maps (RMS errors down to 3 or 4 cm).

Several important applications are made with the cotidal-corange maps.

5 Satellite Altimetry

- Extremely accurate models of oceanic tides are urgently required to allow the correction to satellite radar altimeter measurements of the sea surface height (Geos 3-1975, Seasat-1978, Geosat-1985, ERS-1-1991, Topex-Poseidon-1992). The objective of such measurements is to study ocean variability associated with the meanders and eddies of the major ocean currents (such as the Gulf Stream) and to determine the geoid topography in the oceanic areas, notably above seamounts, trenches and fracture zones.

Such measurements have to rely on the first instance on the presently existing models of ocean tides.

As the Schwiderski cotidal-corange maps are still the best available global ocean tide model (Le Provost et al. 1991), they are used as working standard for all applications as recommended at the IUGG General Assembly in Hamburg in 1983.

However they do not appear to have yet the adequate accuracy (Thomas and Woodworth, 1990) so that altimetry itself is already used to improve them. In 1990, Cartwright and Ray published a direct tidal analysis on the basis of the Geosat first year measurements (1986) which was obtained by using crossover points and positions over which the satellite passed at least twice.

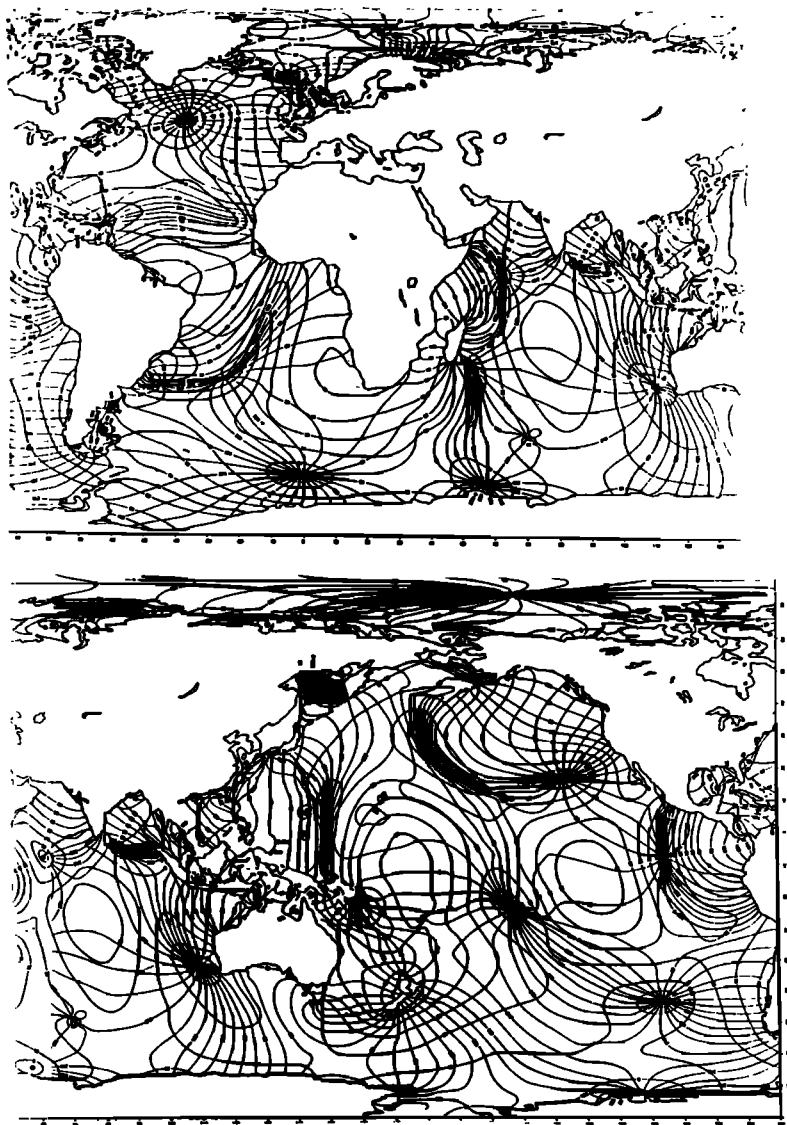


Figure 5: Schwiderski cotidal-corange map for the wave M2.

- Despite the harmonic components are strongly aliased in frequency (exact track repeats every 17 days) all constituents, at the exception of P1, are resolvable within 11 months.

The agreement between Geosat tidal determinations and the Schwiderski maps is remarkably good, within 5 centimeters (see for example M2 in a 1° wide zonal band across the Pacific Ocean - ripple of wavelength 7.5° comes from contamination of the M2 aliased period 317 days with an annual component which is only partly of tidal origin) but there are important areas with 10-15 cm discrepancy and some higher ones (Patagonian shelf, Gulf of Panama).

6 Loading

Another extremely important application of the oceanic tide maps consists in calculating the combined effects of the attraction of the moving water masses and the loading they exert upon the crust. These calculated effects can be compared with observed height, strain, tilt and gravity changes in continental and island observatories.

This necessitates the construction of corresponding Green functions for layered elastic earth models. The convolution of the Green functions $G(\alpha)$ with the oceanic tides $H(\phi', \lambda')$ gives the response $I(\phi, \lambda)$ of the crust.

$$I(\phi, \lambda) = \rho_w \int \int_S G(\alpha) H(\phi' \lambda') dS' \quad (5)$$

$$\alpha = \arccos(\sin \phi \sin \phi' + \cos \phi \cos \phi' \cos(\lambda - \lambda'))$$

α is the angular distance between the application point (ϕ', λ') and the observation point (ϕ, λ) .

Important differences in the tilt Green's functions (Figure 6) appear from different crustal and upper mantle structures at distances closer than 100 km from the load. This may be an efficient tool to improve our knowledge of the crustal structure by using tidal tilt (and strain) observations (Beaumont and Lambert, 1972; Beaumont 1978) providing informations which differ from seismic data: average elastic properties over a loaded area instead of along a path of a seismic ray, independent of the density distribution and corresponding to much lower frequencies potentially useful to investigate inelastic properties.

At distances of several tens of kilometres from the sea the height changes of the crust are generally of the order of one centimetre peak to peak. For islands or a peninsula like Cornwall in England it can reach up to ten centimetres peak to peak (Figure 7). Similarly, gravity changes are of the order of 1 to 2 microgals on the continents and may reach some 10 microgals or more on islands which corresponds to 10% of the direct tidal effect. . A difficulty has appeared with the calculations of gravity changes due to oceanic tides effects because no cotidal-corange map conserves perfectly the mass of the oceans. However this is essential for gravity computations so that it became necessary to redistribute the non negligible masses in excess (sheets of few centimeters covering the oceans) over the whole surface of the oceans either equally, either in function of the tidal amplitudes.

For a given wave (for example M2) the elementary vectorial combination of the observed vector $\bar{A}(A, \alpha)$ with the elastic oceanless earth model response $\bar{R}(R, 0)$ and the oceanic loading and attraction effect $\bar{L}(L, \lambda)$ allows to calculate a residue $\bar{X}(X, \chi)$ (Figure 8) :

$$\bar{A} - \bar{R} - \bar{L} = \bar{X} \quad (6)$$

which should correspond to white noise unless some unidentified effect has been overlooked.

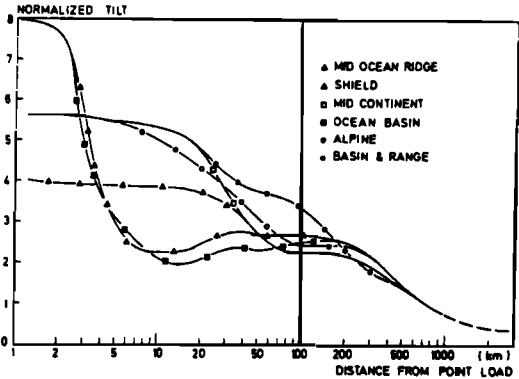


Fig.6 Tilt Green's functions for some major crust and upper mantle models according to Beaumont and Lambert

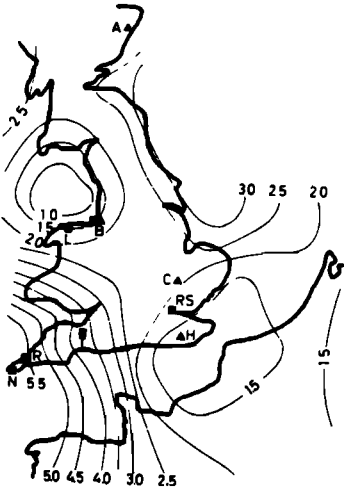


Fig.7 M_2 elastic depression in centimetres due to ocean-tide loading: Boussinesq's solution for plane by Bower (1970), Gravimetric stations at : B (Bidston), L (Llanrwst), N (Newlyn), T (Taunton), R (Redruth), RS (London), A (Aberdeen) , C (Cambridge), H (Herstmonceux)

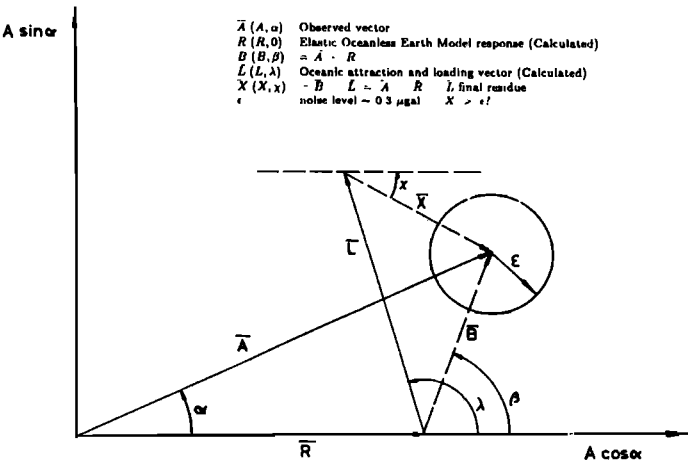


Figure 8: Vectorial representation of the tidal vectors (eqn.6).

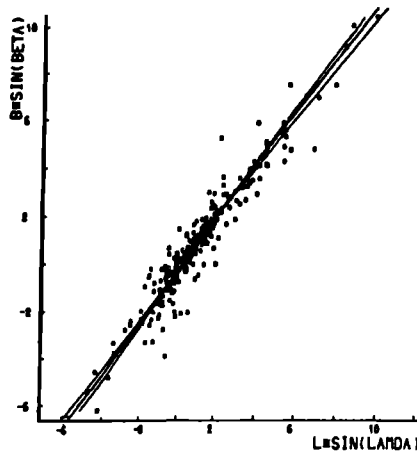


Figure 9:

M_2 Wave: ICET tidal gravity data bank;
 Correlation between vectors \bar{B} and \bar{L} (290 stations)
 $B \sin \beta = -0.207 + 1.049 L \sin \lambda$ (μgal) correlation coefficient: 0.97

As a matter of fact the amplitudes X for 80% of the 325 tidal gravity stations included in the ICET data bank are less than 1 microgal while their mean value, 0.3 microgal, is obviously the limit one can reach with usual spring gravimeters. We must therefore question the existence of few quite larger residues (up to 3 μgal) sometimes observed in excellent stations.

On the other hand the simplest way to evaluate the representativity of one oceanic cotidal map and of the ground based tidal measurements is to correlate the vectors $\bar{B} = \bar{A} - \bar{R}$ and \bar{L} through their cosine and sine components $B \cos \beta$ with $L \cos \lambda$ and $B \sin \beta$ with $L \sin \lambda$. This is shown on Figure 9 and in the Table VI. It clearly appears that the sine correlations are systematically stronger than the cosine correlations which correspond to larger residues. This seems to be due to an imperfect modelling of the solid earth response \bar{R} as this vector affects the cosine component only.

Thus, removing all modelled effects (model earth response and oceanic model load and attraction) from the observations may allow to investigate other suspected effects: inelasticity, lateral heterogeneities, heat flow correlation, dissipation in the core-mantle boundary layer. With this advance we come into controversial interpretations.

In a attempt to recover the oceanic tides by inversion of heterogeneous data (coastal tide gauges, deep sea pressure recorders, gravimeters and satellite altimetry), Francis and Mazzega (1989) made an inverse solution with some 230 "on land" tidal gravity load measurements from the ICET Data Bank. Their solution exhibits the well known features of the oceanic tides, the main amphidromic points being well positioned with the right phase rotations.

However the lack of observations in some continental areas of the northern hemisphere and the poor coverage in the southern hemisphere due to the continental shape, not to mention that the geophysical information content of these data is not fully elucidated, made this application only preliminary even if promising. There is a need for future research on this point.

Table VI
Correlation coefficients between the observed
gravimetric vector \bar{B} and the calculated
oceanic attraction and loading vector \bar{L}

Wave	N	In phase component (cosine)	Out of phase component (sine)
Q1	32	0.776	0.702
O1	175	0.516	0.778
P1	55	0.567	0.720
K1	177	0.459	0.643
N2	171	0.698	0.776
M2	180	0.848	0.929
S2	179	0.717	0.634
K2	53	0.723	0.770

N: number of observing stations
(Melchior and De Becker, 1983)

7 Earth Deceleration

Making a budget of the dissipation effects to control the deceleration of the Earth's rotation in another important goal of cotidal-corange maps.

Astronomical observations of the motion of the Moon in longitude performed for more than 2000 years by even crude optical means have shown that the Earth loses rotational energy; its speed of rotation has decelerated during the last centuries in such a way that, after 100.000 years every day will be longer by 2 seconds of time. Comparison of the situation of centrality lines of total solar eclipses since the Antiquity with their calculated position in the hypothesis of a constant rate of rotation shows a discrepancy in longitude which increases with the square of time. Thus, when we go back 2000 years, the discrepancy reaches 4 hours (Table VII). Here, astronomers need the help of qualified historians to decipher the babylonian, egyptian, greek and chinese documents.

Transits of the planet Mercury on the solar disk and, since some 20 years, Lunar Laser ranging have provided results in good agreement with solar eclipses.

Since the last century measurements of occultations of stars by the Moon have confirmed these numbers.

This secular retardation was also confirmed by palaeontologic data related to growths increments in marine invertebrate. The recent recognition of cyclically laminated tidal rhythmites due to tidal influence on sedimentation provides a new approach to this problem. Late Proterozoic clastic rhythmites (650 million years ago) provide palaeorotational parameters (Williams 1990): at the time, there were 21.9 hours in a day and, consequently, 400 ± 7 days in a year (Table VIII). Here again the cooperation with palaeontologists is essential.

Now similar effects observed on artificial satellite orbits allow to investigate this phenomenon with a highly increased precision.

Kant's idea about the friction of tides was pursued during more than two centuries without succeeding to establish a clear and correct budget between the energy constantly supplied to the oceans by the tide generating forces and the energy lost by eddy dissipation, friction and interactions with the solid earth tide. Considerable divergences have always animated the

the debate between astronomers, oceanographers and geodesists and yet, despite important recent progress, we cannot say that the subject is closed.

Table VII

Length of the day	$LOD = 2\pi/\omega = 86164 \text{ s}$
Rotation rate	$\omega = \omega_0 + \gamma t, \quad \omega_0 = 7,292 \cdot 10^{-5} \text{ rad s}^{-1}$
Secular retardation	$\gamma = d\omega/dt = -4.8 \cdot 10^{-22} \text{ rad s}^{-2} (*)$
	$\frac{d\omega}{\omega_0} = -6.58 \cdot 10^{-18} \text{ s}^{-1} dt$
	If $dt = 100 \text{ years} = 3.2 \cdot 10^9 \text{ s}: \quad d\omega \sim -2.1 \cdot 10^{-8} \omega$
	$\frac{d(LOD)}{LOD} = -\frac{d\omega}{\omega} = 2.1 \cdot 10^{-8}$ thus $d(LOD) = 1.81 \text{ ms per century}$
	Delay, in longitude, after m days: $d\lambda = \frac{1}{2}(\frac{d\omega}{\omega})m^2 \text{ rad}$
	For 2000 years = 730500 days $\Delta\lambda = 0.951 \text{ rad} \simeq 54^\circ \sim 3.6 \text{ hours}$
	$GEM - T_2$ braking is $\gamma = -4.8 \pm 0.32 \cdot 10^{-22} \text{ rad s}^{-2} (*)$
	Eclipse records prior to 1620 $d(LOD) = 2.4 \text{ ms per century} (**)$

(*) Marsh et al., 1990

(**) Stephenson and Morrison, 1984

Table VIII

Late Proterozoic ($\sim 650 \text{ Ma}$) and present tidal and rotational parameters. (G.E. Williams, 1990)

Parameter	Late Proterozoic	Present
Solar days/lunar month	30.5 ± 0.5	29.53
Lunar months/year	13.1 ± 0.1	12.37
Solar days/year	400 ± 7	365.24
Length of solar day (hours)	21.9 ± 0.4	24.00
Earth-Moon distance (R_E)	58.28 ± 0.30	60.27
Lunar retreat rate (cm/year)	1.95 ± 0.29	3.7 ± 0.2

There are two different ways to evaluate the tidal dissipation in the Earth Moon system: the astronomical method and the geophysical method.

The long history of the subject is a permanent contradiction between these two evaluations and a search to reconcile them.

The astronomical method, based upon the rate of deceleration of the Earth's rotation and on orbital perturbations of the Moon and artificial satellites has systematically given a higher amount for the power involved in the tidal distortions and deceleration of the earth's rotation (around 3 Terawatt) than the geophysical estimations (around 1.8 Terawatt). All efforts have aimed at filling the gap.

Diverse geophysical methods have been used: the energy flux as derived from tidal currents (Miller 1966), the friction method using the cotidal-corange maps, and the torque method by simply calculating, through a surface integral, the torque exerted by the East West component of the tidal force upon the tidal height.

Of course many difficulties came from the insufficiently accurate ocean tide models, so we may hope to have now a clearer view of the subject.

At first, on the basis of the most recent results of Seismology, we presently know that the dissipation due to inelasticity of the body of the Earth is far too small to contribute more than few percents to the energy budget of the system (Zschau 1986) so that the quantitative explanation must be searched in the Oceans and more probably in the Ocean-Earth interactions.

Furthermore the eddy dissipation related to turbulence is burned into heat while, as was demonstrated in 1978 by Sündermann and Brosche, the dissipation by molecular viscous friction is lost in heat at the bottom of the ocean and does not contribute to the retardation of the earth rotation. This was confirmed by Schwiderski computations.

Quoting Schwiderski (1983) the physical processes by which the moon interacts with the solid earth through the medium of the ocean's tide is described as follows: "While the moon's gravitational force pulls the earth and ocean tides around in a nonsynchronous fashion, the oceans gear into the tidal distortions of the ocean floor and brake the rotation of the earth with their tidal bottom pressure. In fact, the mean rate of ocean tide bottom pressure work W_p^o provides almost exclusively the power to accomplish the observed deceleration of the earth rotation. As is physically necessary, the braking of the earth is accompanied by tidal friction and, hence, burning of energy in the thin turbulent boundary layer at the ocean floor. It is remarkable that the oceanic tidal braking of the earth costs about 53% heat loss of the moon's total gravitational ocean tide energy supply and converts only 47% into a loss of rotational energy of the earth" (see also similar result in Platzman, 1984). One should note that this proportion do not depend upon any oceanic cotidal- corange model but on the fact that such a pressure effect is proportional to the height of the bottom earth tide, thus to the h_2 Love number, and inversely proportional to the applied potential, thus to $1 + k_2$ Love number. The ratio $h_2/(1 + k_2)$ is 0.47.

Quantitatively, on the basis of his M2 cotidal-corange map, Schwiderski obtains 3.55084 TW (1 Terawatt = 10^{12} watts) as the mean rate of gravitational work on the oceans, a loss by mean rate of bottom pressure work of 1.66906 TW, a loss by bottom friction of 1.87741 TW ¹ and a mean rate of eddy dissipation work in oceans of 0.00436 TW only ². This perfectly equilibrated budget follows by identical operations and expresses only the fact that the equations have been

¹1.27 TW come from shelf areas in agreement with Miller estimation (1966), 0.41 TW from slope areas in agreement with Munk estimation and 0.20 TW from deep seas.

²Platzman (1984) obtains 1.93 TW for M2, 0.21 TW for S2, *1.74 TW being transferred to the lithosphere of which 0.03 TW is dissipated in the solid earth and 1.71 TW returned to the Moon: the solid earth works on the Moon at this rate".

properly integrated.

However in this scheme, the conservation of Energy in the closed moon-ocean- earth system result in a serious deficit so that, contrarily to all observations, the moon would be accelerated on its orbit ($\dot{n} = +46'' \text{cy}^{-2}$).

According to Schwiderski it is only possible to fit the astronomical observations by introducing an earth tide phase lag ϵ of 0.45° .

The introduction of this earth tide phase lag practically does not change the torque exerted by the oceanic tide pressure ($-23.8 \cdot 10^{15}$ joule) but it introduces an additional gravitation torque, proportional to the Love number h and to the sine of ϵ ($-4.6 \cdot 10^{15}$ joule for $\epsilon = 0.5^\circ$), thus satisfying the energy conservation law. It must be emphasized that for Schwiderski, this phase lag should not be attributed to internal dissipation, but to the tidal interaction due to the pressure exerted by the oceanic tide upon the tidally deformed bottom of the oceans. However Zschau (personal communication, 1991) shows that the ocean tide bottom pressure on the body tide ($h_2/(1+k_2) = 0.47$) is balanced by the gravitational work of the loading tide on the moon ($-k'_2/(1+k_2) = 0.24$) and the gravitational work of the body tide on the ocean tide ($k_2/(1+k_2) = 0.23$), this resulting from the equality $h_2 = k_2 - k'_2$. Consequently Zschau considers the braking as due to the pressure of the ocean tide bulge on the coast lines.

On the basis of the law of conservation of angular momentum in the Earth-Moon system it is obvious that in order to compensate the loss of earth spin angular momentum, we must observe a corresponding increase of the Moon's angular momentum which can be obtained only by an increase of the Earth Moon distance a . By virtue of Kepler's 3rd Law ($n^2 a^3 = G(M+m)$) we should observe a deceleration of the mean motion n of the Moon:

$$\frac{da}{dt} = -\frac{2a}{3n} \frac{dn}{dt} \quad (7)$$

We can thus consider that, in the energy budget of the Earth-Moon system there is a decrease of the kinetic energy of rotation of the Earth, a decrease in the kinetic energy of the respective orbital movements of the Earth and the Moon, and an increase of the gravitational potential energy of the two bodies system.

The deceleration of the mean motion n of the Moon is observable but the results of classical optical astronomy suffered from considerable scatter which made them very uncertain.

The results obtained by laser ranging on the reflectors deposited on the lunar surface by the Apollo and Luna missions since 1969 have recently provided an excellent determination

$$\dot{n} = (-26.1 \pm 1.0)'' \text{cy}^{-2} \quad (\text{Dickey et al. 1990}) \quad (8)$$

in perfect agreement with those derived previously from the planet Mercury transits on the solar disk:

$$\dot{n} = (-26.0 \pm 2.0)'' \text{cy}^{-2} \quad (\text{Morrison and Ward, 1975}) \quad (9)$$

so that, from eqn (7), one derives

$$\dot{a} = +3.6 \text{ cm year}^{-1} \quad (10)$$

the rate of recession of the Moon from the Earth.

Now, like the Moon, the artificial satellites trajectories are perturbed by the redistribution of masses resulting from the tides in the Earth and Oceans. These perturbations are observable as long period variations of the inclination and node of their orbits (Figure 10) and also of the semi major axis and the excentricity (Table IX, Lambeck 1977).

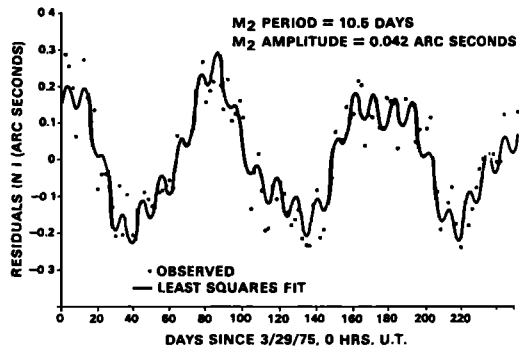


Figure 10: Residuals in inclination for Starlette. (Felsentreger et al. 1979)

Table IX
Importance of the four main tidal deformations on the
satellite orbits according to Lambeck (1977)

		Sectorial Waves		Tesseral Waves (declinational)	
		M2	N2	O1	K1
semi major axis	$\dot{a}(\dot{n}^*)$	80%	4.5%	14.3%	0
excentricity	\dot{e}	-7%	91 %	16 %	0
inclination	\dot{i}	81 %	3 %	-70.3 %	79 %

N2 is an "elliptic" wave of M2 and has a major role on e
O1 and K1 are declinational waves of opposite sign
K1 is luni-solar (66% from the Moon)
K1 tidal bulge is permanently oriented towards the vernal equinox
(*) \dot{n} is a consequence of \dot{a}

Of course, the satellites do not undergo perturbations at the diurnal and semi-diurnal tidal frequencies which result from the rotation of the earth. What they see is the orientation of the tidal bulges with respect to space. Thus, the frequency of the perturbations is obtained by subtracting the sidereal frequency of rotation of the earth from the tidal frequency, just like for precession-nutations, and obviously by subtracting the frequency of the node retrogradation of the satellite's orbital plane in space. This yields periods

$$T_i(D) = 2\pi/(\omega - \omega_i - \dot{\Omega}) \quad \text{for diurnal tides} \tag{11}$$

$$T_i(SD) = 2\pi/(2\omega - \omega_i - 2\dot{\Omega}) \quad \text{for semi diurnal tides} \tag{12}$$

The K1 tide ($\omega_i = \omega$) results in long or even extremely long periods in the case of polar orbits where $\dot{\Omega} \sim 0$ while M_2 and O_1 yield periods around 13.6 days which are difficult to discriminate (Table X).

Table X

	a(km)	i	$\dot{\omega}$ /day	K1		O1		P1		M2		S2	
				σ_i	T_i	σ_i	T_i	σ_i	T_i	σ_i	T_i	σ_i	T_i
BE-C	7 502 200	41°19	-4.2535°	-4.25°	85	30.60°	11.7	6.22°	57.9	34.85°	10.3	10.47°	34.4
Starlette	7 300 000	49°80	-4.00°	-4.00°	90	30.35°	11.9	5.97°	60.3	34.35°	10.5	9.97°	36.1
Geos-1	8 072 900	59°38	-2.2465°	-2.25°	160	28.60°	12.6	4.17°	86.3	30.85°	11.7	6.47°	55.8
Transit 67	7 453 770	89°30	-0°072	-0°072	5000(±)	26.43°	13.6	2.04°	176.0	26.50°	13.6	2.12°	170.0
Geos 2	7 705 000	105°79	+1.40°	+1.40°	257	24.95°	14.4	0.57°	631.0	23.55°	15.3	0.83°	434.0
Geos 3	7 220 000	114°98	+2.73°	+2.73°	132	23.62°	15.2	-0.76°	474.0	20.89°	17.2	3.49°	103.0
Seasat	7 171 000	108°02	+2.02°	+2.02°	178	24.33°	14.8	-0.05°	7130(±±)	22.31°	16.1	2.07°	173.9
Geosat	7 162 600	108°00											

The frequencies σ_i are given in degrees per day.
The periods $T_i = 2\pi/\sigma_i$ are given in days.

- (±) Polar satellites like Transit 1967.92A having $\dot{\Omega} \sim 0$, do not allow to separate the main lunar waves O1 and M2 (13.6 days period) which however have a totally different behaviour in the solid earth tide and even more in the oceanic tides. Similarly P1 cannot be separated from S2. K1 wave is "frozen".
- (±±) These satellites are sun-synchronous so that the P1 wave is "frozen".

To evaluate the quality of a cotidal-corange oceanic map by comparison with the perturbations of artificial satellites it is appropriate to expand the oceanic tidal height of every component in a Fourier spherical harmonic expansion which yields, for example, in the case of the Schwiderski M_2 tide:

$$\zeta = \sum_{n=0}^{\infty} \sum_{m=0}^n |C_{nm}^{\pm} \sin(\sigma t + \chi + \epsilon_{nm}^{\pm} \pm m\lambda)| P_n^m(\cos \theta) \quad (13)$$

$$C_{22}^+ = 2.95 \text{ cm} \quad \epsilon_{22}^+ = 311.6^\circ \quad (14)$$

One may then compare these parameters with those deduced from satellite solutions:

$$C_{22}^+ = (3.24 \pm 0.13) \text{ cm} \quad \epsilon_{22}^+ = 328^\circ \pm 2.5^\circ \quad (\text{Zschau 1986}) \quad (15)$$

These are average of solutions obtained with Starlette, Geos 3 and three Transit satellites from 1977 to 1982.

This result corresponds of course to the global effect of oceanic tides, earth tides and their interactions, and contains the contributions not only of M_2 but also of O_1 and N_2 .

To derive a C_{22} coefficient representative of the ocean tide from the satellite perturbations, the earth tide effect, usually modelled with $k = 0.3$, $\alpha = 0^\circ$, must be subtracted. It was shown by Goad and Douglas (1978) that an earth tides phase lag α equal to 0.5° reduces C_{22}^+ by almost 0.5 cm (3.23 to 2.76).

Lambeck has shown (1975) that the C_{22} , ϵ_{22} tidal parameters which correspond to a layer of salt water density 1.03 can be used directly to calculate the gravitational effects of the oceans on the evolution of the orbit of the Moon that is the increase of the Earth Moon distance a and, as a consequence, the deceleration of its mean motion \dot{n} :

$$\begin{aligned} \dot{n} = & -843(k_2 \sin \epsilon)(M_2) - 151(k_2 \sin \epsilon)(O_1) - 47(k_2 \sin \epsilon)(N_2) \text{ solid Earth tides} \quad (16) \\ & -7.81(C_{22}^+ \cos \epsilon_{22}^+)(M_2) - 1.63(C_{21}^+ \sin \epsilon_{21}^+)(O_1) - 2.25(C_{22}^+ \cos \epsilon_{22}^+)(N_2) \text{ ocean tides} \end{aligned}$$

(Cazenave, 1982).

These equations also include contributions of the oceanic tides O_1 and N_2 which are practically the only important ones besides M_2 (Table IX). They were found in this way:

a) from laser ranging on Starlette and Lageos satellites

$$\dot{n} = (-25.5 \pm 1.25)'' \text{ cy}^{-2} \quad (\text{Cazenave 1982}) \quad (17)$$

b) from the Goddard Earth Model GEM-T2 tidal constituents

$$\dot{n} = (-26.04 \pm 0.51)'' \text{ cy}^{-2} \quad (\text{Marsh et al. 1990}) \quad (18)$$

exactly the same as measured by Lunar Laser Ranging (eqn.8) which should mean that the dissipation inside the Moon is negligible at this level of precision, in agreement with studies of lunar seismicity.

The other way to treat the problem is of course to subtract the oceanic contribution to dissipation (eqn. 14) from the satellite data (eqn. 15) to try to evaluate the contribution of the solid earth. This view was developed by Zschau (1986).

Recalculating the tidal energy flux on the basis of the satellite perturbations by the M_2 tide (C_{22} , ϵ_{22} in eqn (15), this author obtains a total M_2 tide dissipation rate of

$$\dot{E} = [2.69 \pm 0.13] \text{ TW} \quad (19)$$

with a global phase delay of $5.32^\circ \pm 0.26^\circ$ (oceans and solid earth). Subtracting the ocean tide

dissipation calculated on the basis of the best recent oceanic tide models, he tries to identify the residue of the solid Earth dissipation rate for the M2 body tide which is proportional to the product $k \sin \epsilon$ (k second Love number, ϵ phase lag). He then derives these two parameters characterizing the rheology of the Earth which are not independent from each other because they characterize inelastic processes in the mantle which have causal properties (Zschau 1986): for the Parke Hendershott cotidal map

$$\begin{aligned} C_{22} &= 3.38 \text{ cm} & \epsilon_{22} &= 313.1^\circ \\ k &= 0.3073 \pm 0.0013 \\ \epsilon &= 0.78^\circ \pm 0.24^\circ \end{aligned} \quad (20)$$

for the Schwiderski cotidal map

$$\begin{aligned} C_{22} &= 2.95 & \epsilon_{22} &= 311.6^\circ \\ k &= 0.3048 \pm 0.0013 \\ \epsilon &= 1.24^\circ \pm 0.24^\circ \end{aligned} \quad (21)$$

However the error in the satellite solutions is about 5% of the total dissipation rate while the spread between different ocean tide models is even larger and corresponds to the likely earth tide contribution.

Considering these large uncertainties, Zschau has tried to make use of the Chandler polar wobble quality factor Q to evaluate the tidal friction in the solid earth. He concludes that the real significance of his results is not certain because the frequency dependence of the specific dissipation function Q^{-1} in the Earth's mantle is practically unknown.

A power law $Q \sim \omega^\alpha$ is commonly proposed to adjust seismic data with the Chandler polar wobble (period 434 days) but the reference frequencies of Q determinations in the seismological frequency band are often unclear while the α value is badly known ($\alpha = 0.3?$).

It is therefore still impossible to reliably estimate in this way the solid Earth tidal dissipation (with $\alpha = 0.3$ the solid earth dissipation would amount to 50% of the total rate). The constraints from the Chandler wobble period ($433.3 < \tau < 436$ days observed) show that $\alpha \geq 0.3$ can be ruled out as it gives $\tau = 452$ days or more.

The "most probable" results then proposed by Zschau for the M2 wave were: a solid earth dissipation $E_{SE} = 0.12 \text{ TW} = 4.4\%$ and a solid earth phase delay $\epsilon = 0.21^\circ$.

However, more recently, Dehant and Zschau (1989) put an upper limit of 0.005° for the solid earth tide, on the basis of the seismically sound earth models.

8 Precession - Nutations

Precession and nutations result from gravitational interactions of the Earth, Sun and Moon.

The torques producing precession and nutations are exerted by the tesseral diurnal tidal forces.

However precession and nutations are movements of the axis of figure of the Earth described in an inertial system of fixed axes, while tides are observed at points fixed with respect to the rotating Earth.

It results that the frequency of a nutation can be directly deduced from the frequency of the corresponding tide by subtraction of the sidereal frequency (15.041° per hour UT).

The total torque exerted on the planet is

$$\bar{N} = \int \int \int_v (\bar{r} \wedge \overline{\text{grad}W}) \rho \, dv \quad (22)$$

This integral, extended to the entire volume of the planet, is transformed to

$$\bar{N} = - \int \int \int_v \text{rot} (\rho W \bar{r}) \, dv - \int \int \int_v (\bar{r} \wedge \overline{\text{grad}\rho}) W \, dv \quad (23)$$

and, using the Ostrogradsky theorem:

$$\bar{N} = - \int_s (\bar{n} \wedge \bar{R}) \rho W \, dS - \int \int \int_v (\bar{r} \wedge \overline{\text{grad}\rho}) W \, dv \quad (24)$$

where \bar{R} is the vectorial radius at the external surface and \bar{n} is the external normal (Melchior 1982).

The first term is zero in the case of a spherical Earth ($\bar{n} // \bar{R}$) (effect of geometrical ellipticity) while the second term is zero for a density distribution of spherical symmetry ($\bar{r} // \overline{\text{grad}\rho}$) (effect of dynamical ellipticity). A surface integral term exists for every surface of discontinuity of ρ .

An elementary graphical representation of the distribution of the north-south component of the tidal force along a meridian plane of an ellipsoidal Earth shows how the tesseral tidal force exerts a torque about an axis perpendicular to the axis of figure. This torque makes the equator sway towards the ecliptic (Figure 11). However the contribution of the east-west component and the gyroscopic effect of the Earth's rotation need to be taken into account for a

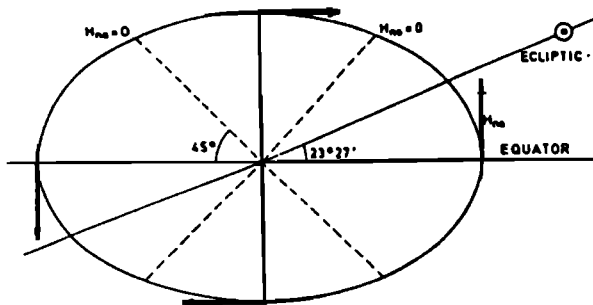


Figure 11: Torques produced on an elliptic Earth by the North-South component of the tidal forces.

correct derivation of precession-nutations from the tidal potential. The main luni-solar diurnal tidal wave called K1 has a sidereal frequency ω ; it corresponds to a bulge directed towards the vernal equinox. Subtracting the sidereal frequency ω gives zero, that is a secular movement of the axis which is the circular luni-solar precession of the equinox.

$$\Psi = -E \frac{\omega A(K_1)}{\sin \theta} = -50'' 38 \text{ per year} \quad (25)$$

On the other hand tidal spectral lines are distributed symmetrically with respect to the K1 sidereal frequency ($\omega + \Delta\omega_i$ and $\omega - \Delta\omega_i$) so that when operating the subtraction of ω one obtains pairs of circular nutations of same frequency $\Delta\omega_i$ but of opposite sign (prograde for $-\Delta\omega_i$, retrograde for $+\Delta\omega_i$).

An elliptical nutation is the result of the combination of each pair of opposite circular nutations.

Introducing the tidal potential development as given by eqn.(1) into eqn. (24) shows that precession and nutations are produced only by tesseral terms $n = 2$, $m = 1$ and after some calculations, yields for the luni-solar precession and the astronomical elliptical nutations of the rigid earth:

$$\begin{aligned} \Delta\theta &= -E \sum_i \frac{\omega}{\Delta\omega_i} (A_i - A_{-i}) \cos(\Delta\omega_i t) \\ \sin \theta \Delta\Psi &= -E \sum_i \frac{\omega}{\Delta\omega_i} (A_i + A_{-i}) \sin(\Delta\omega_i t) \end{aligned} \quad (26)$$

(θ is the obliquity of the ecliptic $23^\circ 27'$ and $E = \frac{3}{2} \frac{GM}{c^2} \frac{C-A}{C\omega^2} = 0'' 016443$).

During 75 years, from Kelvin to Takeuchi, all attempts to evaluate the elastic response of the Earth to tidal forces (Herglotz, Prey, Boaga, Jeffreys) were conducted by using extremely crude earth models and only Takeuchi succeeded to perform a numerical integration of the differential equations with desktop computers.

These models were the so-called SNREI models: spherically stratified, non rotating, elastic, isotropic.

Serious analytical difficulties appear indeed with the Coriolis force due to the rotation and with the ellipticity of the surfaces.

These difficulties were addressed step by step: Poincaré (1910) introduced an ellipsoidal rotating non viscous liquid core within a rigid mantle; Jeffreys and Vicente (1957), Molodensky (1961) used an elastic non rotating mantle, considered rotation and ellipsoidal stratification only within the fluid core and imposed serious restrictions on the form of fluid motions in the core.

The earth model which has been used more recently was a planet which is hydrostatically pre-stressed, self gravitating, rotating, inelastic and where slightly ellipsoidal equipotential surfaces coincide with surfaces of equal density and rheological parameters.

The general vectorial field of displacements combines

- a spheroidal field S_m^n which is defined by prescribing the form of two scalar functions of the radius

$$\bar{\sigma} = \sum_{n=0}^{\infty} \sum_{m=0}^n [r U_n^m(r) Y_n^m + V_n^m(r) \bar{\nabla}_1 Y_n^m] \quad (27)$$

$$\nabla_1 = \theta \frac{\partial}{\partial \theta} + \lambda \frac{\partial}{\sin \theta \partial \lambda} \quad \text{gradient operator on the unit sphere} \quad (28)$$

- a toroidal vectorial field T_n^m which is defined by prescribing the form of one scalar function of the radius

$$\bar{r} = \sum_{n=0}^{\infty} \sum_{m=0}^n W_n^m(r) [-r \wedge \nabla_1 Y_n^m] \quad (29)$$

so that the displacement components to be introduced in the fundamental equations are

$$\begin{aligned} u_r &= \sum_n \sum_m U_n^m(r) P_n^m(\cos \theta) \cos(\omega_i t - m\lambda) \\ u_\theta &= \sum_n \sum_m V_n^m(r) \frac{\partial}{\partial \theta} P_n^m(\cos \theta) \cos(\omega_i t - m\lambda) \\ &\quad - \sum_n \sum_m m W_n^m(r) \frac{1}{\sin \theta} P_n^m(\cos \theta) \cos(\omega_i t - m\lambda) \\ u_\lambda &= \sum_n \sum_m m V_n^m(r) \frac{1}{\sin \theta} P_n^m(\cos \theta) \sin(\omega_i t - m\lambda) \\ &\quad - \sum_n \sum_m W_n^m(r) \frac{\partial}{\partial \theta} P_n^m(\cos \theta) \sin(\omega_i t - m\lambda) \end{aligned} \quad (30)$$

Taking into account the rotation of the earth means that one has to introduce the Coriolis force in the first term of the Navier Stokes equations, that is for example in the radial component:

$$\frac{\partial^2 u_r}{\partial t^2} - 2\omega \sin \theta \frac{\partial u_\lambda}{\partial t} \dots \quad (31)$$

A quick look at the equations (30) shows that the derivative of the Legendre polynomial P_n^m with respect to the colatitude θ which contributes to the toroidal part of u_λ introduces in the equation (31) the P_{n-1}^m and P_{n+1}^m polynomials.

It results that toroidal modes r_{n-1}^m and r_{n+1}^m become coupled with the basic spheroidal tidal mode S_n^m .

Consideration of the ellipsoidal figure of the planet has a similar effect.

This had been anticipated by Love in 1911 who gave even the theoretical form of the correction (polynomial Y_4^1 combined with the classical Y_2^1) and estimated that the correction should be of the order of ellipticity (1/300) thus negligible at his time.

The development of the complete theory was initiated by Dalhen (1968) Smith (1974), Crossley (1975), Shen (1975), Shen and Mansinha (1976) and fully extended in a series of six beautiful papers by Wahr (1981) with Smith and Sasao which constitute a comprehensive treatment of all aspects of the motion of an oceanless elastic earth.

The effect of ellipticity and rotation is thus to bring a coupling between spheroidal and toroidal fields of the same order but different degrees so that an eigenfunction has a displacement of the form of a chain

$$u = \sigma_n^m + r_{n+1}^m + \sigma_{n+2}^m + r_{n+3}^m + \dots \quad (32)$$

For a non-rotating spherically symmetric earth (SNREI model) the absence of the Coriolis term in equation (31) and of the effect of the ellipticity resulted in no coupling of any σ_n^m or r_n^m to any other r_n^m or σ_n^m and made the solution of the differential equations easily tractable with a purely spheroidal tidal displacement $u = \sigma_1^m$.

Now, to make possible the solution of the differential equations the chain (32) obviously has to be truncated, an operation which may introduce errors which only a comparison with high precision observations can appreciate.

In practice a truncated solution for the tesseral diurnal waves

$$u = \tau_1^1 + \sigma_2^1 + \tau_3^1 \quad (33)$$

has been first constructed and, when found, a first order perturbation scheme is used to extend the results to σ_4^1 (Wahr, 1981).

9 The role of the Earth's Core

The τ_1^1 toroidal mode represents a rigid rotation about an axis perpendicular to Oz, the mean axis of the Earth rotation: it is the astronomical precession-nutation.

The response of the earth to the second order tesseral tidal potential ($m=2, n=1$) is strongly frequency dependent because the nutational modes of the mantle excite a differential rotation of the fluid core with respect to the mantle with an eigenfrequency in the middle of the diurnal tidal band. This mode is called the free core nutation: it is a retrograde toroidal motion of the entire outer core (like a rigid rotation), resonantly excited, and it includes important deformations of the core mantle boundary making the body tide as well as the associated astronomical forced nutations resonant.

Two other (2,1) modes have been well documented over many years: the tilt over mode which affects only the forced nutation but not the body tide (no accompanying deformation) and the Chandler wobble astronomically observed for over a century.

Recently, considering possible independent motions of the solid inner core, Mathews et al. (1991) identified two new frequencies which are determined by the dynamical ellipticity of the inner core and the strength of coupling it to the other parts of the Earth by gravitational forces and fluid flow pressure.

They found a prograde inner core wobble which do not contribute to the body tide and a prograde diurnal free inner core nutation, also found by De Vries and Wahr (1991) and by Dehant et al. (1991) (Figure 12) with an eigenfrequency on the other side of the sidereal frequency ($15.0095^\circ \text{ h}^{-1}$ for PREM or $15.0118^\circ \text{ h}^{-1}$ for 1066A - periods of 475.5 and 512.2 days in space, (471 days according to De Vries and Wahr), thus also in the middle of the tidal diurnal band. Its resonance impact is practically negligible on the tides.

One will easily understand that the resonant frequency at which the liquid core can have a nutation with respect to the solid mantle or inner core depends essentially upon the flattening of the core-mantle and inner core boundaries. If the rotating planet is in hydrostatic equilibrium, the flattening of ellipsoidal strata obeys the second order differential equation of Clairaut, the numerical integration of which yields a core-mantle boundary flattening equal to $1/392.8$

The experimental detection of the nearly diurnal free wobble or free core retrograde nutation is problematic and many attempts to discover it directly from astronomical observations were not conclusive. As a matter of fact, one can expect that, being excited by different non securely identified mechanisms its phase and amplitude must be eminently variable.

Therefore, only indirect evidence of it can come from observed resonance in the diurnal Earth tides and in their associated forced nutations.

The analysis of these measurements provides a new tool to investigate the structure and dynamics of the earth liquid core and inner core.

On the basis of the earth models with a core hydrostatic flattening $1/392.8$, the calculated eigenfrequency is found by Wahr (1981) to be $\omega_F = 15^\circ 07' 37.67''$ per hour, that is a period of 23h52m57s (solar) (corresponding to $1/1 + 1/459$ cycle per sidereal day) while the principal tidal diurnal waves have periods and frequencies as given in the Table XII.

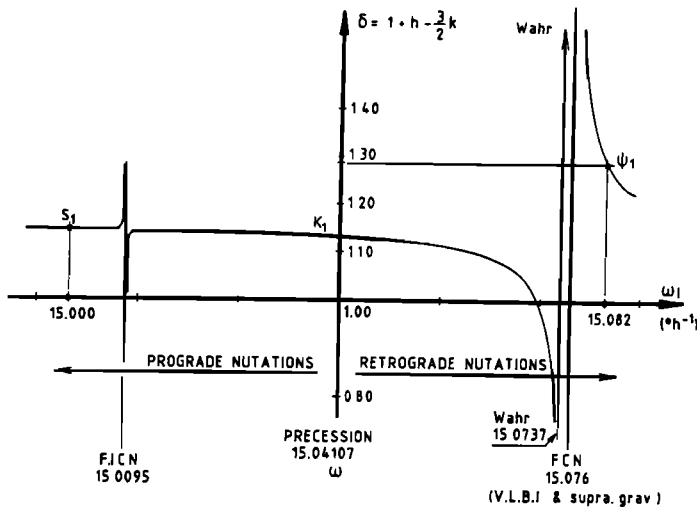


Figure 12:

Eigenfrequencies ω_i of free core (F.C.N.) and free inner core (F.I.C.N.) nutations (Dehant et al. 1991).

Thus, amongst the largest tides, K1 is the nearest to resonance but there is a very small (unfortunately) wave which is much closer to the resonance: ψ_1 elliptic wave of the solar part in K1 with a frequency 15°08213530/hour (Table XII).

The nutations associated with the P1, O1 and ψ_1 waves have frequencies

$$\Delta\omega_i = \omega_i - \omega, \quad (34)$$

given in Table XII, the first two being prograde and the third retrograde. Their associated waves, respectively ϕ_1 , OO1 and S_1 , symmetric to K_1 , give the same periods with opposite signs. The elastic response of the earth models to tidal forces are described by the dimensionless Love numbers from which one derives that the amplitudes of tidal variations of the gravity vector have to be multiplied by a different combination of these Love numbers whether we consider variations in the direction (tilt: factor $\gamma = 1 + k - h$; see Table V) or variations of the intensity (gravity: factor $\delta = 1 + h - \frac{3}{2}k$; see Table XI).

As mentioned previously, there is presently no hope of further research with tiltmeters since the new gravimeters benefit from the absence of site effects and a higher signal to noise ratio.

Like the tiltmeters in 1960, the current spring gravimeters, installed in specially careful conditions have confirmed the resonance effect between O1, P1 and K1 waves:

Table XI. Tidal variations of gravity

Theoretical Amplitude at 50° latitude	Observed amplitude factors δ
O1 30.455 μgal	1.157
P1 14.145	1.157
K1 42.827	1.145

but did not, in general, yield conclusive results for the ψ_1 wave whose amplitude is only 0.342 microgal at 50° latitude, which corresponds to the noise level of such instruments.

The installation of cryogenic gravimeters built by Goodkind Warburton and Reineman in two, later in three, permanent stations in Western Europe gave a decisive impulse to search these core hydrodynamical effects and enabled to evaluate experimentally, for the first time, with a high degree of precision, the resonant frequency.

Table XII

Calculated Eigenfrequency with a core hydrostatic flattening 1/392			
$\omega_F = 15.073767^0/\text{hour}$		Period 23h52m57s (solar)	
<u>Principal tidal diurnal waves</u>			
		Frequency	Period
K1	luni-solar sidereal wave	15.04106063 ⁰ /hour	-23h56m04s (solar)
P1	solar principal wave	14.95893136 ⁰ /hour	-24h03m57s
O1	lunar principal wave	13.94303557 ⁰ /hour	-25h49m09s
ψ_1	elliptic wave of	15.08213530 ⁰ /hour	-23h52m09s
K1 solar part			
<u>Associated astronomical nutations</u>			
K1	15.04106363 ⁰ - 15.04106863 ⁰ =	0	secular (precession)
P1	14.95893136 ⁰ - 15.04106863 ⁰ =	-0.08213727 ⁰	period 182.621116 prograde
O1	13.94303557 ⁰ - 15.04106863 ⁰ =	-1.09803263 ⁰	period 13.660790 prograde
ψ_1	15.08213530 ⁰ - 15.04106863 ⁰ =	0.04106667 ⁰	period 365.259710 retrograde
calculated			
ω_F	15.07376700 ⁰ - 15.04106863 ⁰ =	0.03269837 ⁰	period 458.74 retrograde
solar days			
<u>Observed eigenfrequency</u>			
VLBI		15.07587 ⁰ /hour	
Superconducting gravimeters (Bruxelles + Frankfurt)		15.07590 ⁰ /hour	
From which			
15.0759 ⁰ - 15.04106863 ⁰		period 430.7 solar days, retrograde	

Analyzing the results of three years worth of data obtained in Bruxelles and in Bad Homburg by a stacking method, Neuberg, Zörn and Hinderer obtained (1987):

$$\text{Bruxelles} \quad \omega_F = (15.0760 \pm 0.0009)^{\circ} h^{-1} \text{ or } T = 430 \pm 12 \text{ solar days}$$

$$\text{Bad Homburg} \quad \omega_F = (15.0759 \pm 0.0006)^{\circ} h^{-1} \text{ or } T = 431 \pm 8 \text{ solar days}$$

retrograde motion as $\omega_F > \omega$, with a mean Q value 2781 ± 543 .

This result is in surprisingly good agreement with the results obtained for the corresponding astronomical nutations by Very Long Base Interferometry determinations.

Very long base interferometry allows to measure the differences in arrival times at two (or more) radio telescopes ³ of signals from extragalactic sources (80 radio sources are used by Herring et al. 1991).

These differences depend of course upon the orientation in space (and length) of the chord joining the two radiotelescopes and this orientation reflects the nutations and twistings of

³ Westford, Ft Davis, Richmond in USA, Wettzell in Germany

the earth during its rotation. The extremely high precision of VLBI allows to check angular directions in space with a precision of 10^{-4} arcsecond or better.

Analyzing 798 experiments made from 1980 to 1989, between North America and Europe, Herring, Buffet, Mathews and Shapiro (1991) determined residues with respect to the Wahr series of nutations which was used in their reductions.

The analysis of these residues in frequency and phase gave a non negligible correction for the annual nutation (365.259710 solar days) associated to the ψ_1 wave.

They came to the conclusion that the very high precision of VLBI measurements of the principal nutations terms (0.04 milliarc second on the semi annual nutation $-1''$ is 31 meters at the earth's surface, thus 0.04 mas corresponds to one millimeter!) can be satisfied if two essential parameters of the current seismological earth models are corrected.

It turns out that the spheroidal models constructed on the basis of the spherically symmetric models (PREM, 1066A) by using the Clairaut differential equation to calculate the flattening in function of the radius vector imply hydrostaticity.

Instead of the actual ellipticity of the Earth ($1/298.25$) these models give about $1/299.8$ and a corresponding dynamical flattening $(C-A)/A$ equal to 0.0032472 (PREM) or 0.0032495 (1066A).

The VLBI astronomically observed value is 0.003284915 (Kinoshita value is 0.003284706). This introduces an error of about 1% on the nutation amplitudes which are, in principle, proportional to this dynamical flattening.

Mathews et al. (1991) have introduced this correction. Moreover, to constrain the amplitude of the resonant retrograde annual nutation (corresponding to the tidal wave ψ_1) to fit with the VLBI results ($0''002$ discrepancy), they also increase the hydrostatically determined core flattening (8.87 km or $1/392.46$) by 430 meters (9.30 km or $1/375.235$).

Then, only the prograde fortnightly amplitude is not yet satisfied with this procedure. Dehant (1990) has suggested an effect due to some extra pressure at the core-mantle boundary.

The increase of the core flattening modifies the Wahr resonant frequency $15.0737288^\circ h^{-1}$ to $15.07596872 h^{-1}$ corresponding to $(1/1 + 1/429.8)$ cycle per solar day to be compared with the period of 430.5 solar days given by the two superconducting gravimeters based in Europe.

Inelasticity of the mantle which was taken into account by Dehant and by Wahr cannot account at all for such a difference.

By increasing the flattening one evidently increases the pressure coupling between Core and Mantle and consequently decrease the free period.

Other tentatives were made to look at possible effects of the liquid core stratification as described by the Brunt Väisälä frequency, but earth tides and nutations observational results cannot distinguish between the different hypothesis.

10 Core Decoupling

There is much interest in the elastic response of the Earth to the zonal tidal forces inducing periodic changes of the earth's flattening, thus of the polar principal moment of inertia and, as a consequence of the conservation of angular momentum, to periodic variations of the earth rotation rate ω .

Initially, this was of great importance for the construction of a uniform time scale based upon astronomical observations.

The identification of the principal periods which are 13.66 and 27.55 days for the lunar tides Mf and Mm in the rotational UT1 time scale compared to atomic time scale is straightforward

even with classical optical astronomical observations. According to these observations, the monthly Mm tide seemed to be in better agreement with the calculated effects for an oceanless rigid earth. The fortnightly Mf tide gave a 6% higher response while there were important time fluctuations observed in the responses. However analysis based upon the USSR Standard Time system for 1955-1974 yields estimates of the second Love number k in perfect agreement between themselves (Gubanov and Yagudin, 1978).

Data obtained since 1977 from satellite laser ranging and VLBI ⁴ offer evidently a considerable improvement in precision (Hefty and Capitaine 1990). Moreover it is now possible to correct the daily values for the atmospheric angular momentum effect before evaluating the Mf and Mm responses.

This result is a noticeable improvement because there is sufficient power, due to zonal winds, to corrupt the data principally at the monthly period.

Correction for equilibrium ocean response is applied and it is noted that the Schwiderski dynamical model gives only negligible difference with respect to the equilibrium response (Merriam 1985).

However, applying these atmospheric and oceanic corrections did not resolve the discrepancies with respect to theoretical models.

Considering that the viscosity of the Earth's liquid core is so small, it was then proposed to consider that this fluid core, which contributes to about 10% in the change of rotation, cannot follow the "quick" monthly variations in the mantle's rotation rate so that it is decoupled from the mantle at these frequencies (Merriam 1980, Wahr et al. 1981) that is at periods up to one month at least.

This of course satisfies the astronomical observations but it has important consequences. If there is a periodic differential rotation between core and mantle so that each part conserves angular momentum separately, there is a velocity discontinuity at their interface. This was estimated to $4.10^{-5} \text{ cm s}^{-1}$ by Wahr et al. that is, by far (10^{-3}), much less than what is required by the westward drift of the magnetic field.

However, this raises the question of a weak viscous coupling and dissipation in the thin boundary layer at the core mantle boundary. If this effect could be detected with precision we should have, like in the case of nutations, a new tool to investigate dissipative processes within the core.

Very unfortunately this effect seems to be so small that it could only be detected on cumulative very long period effects; for example on the 18.6 years lunar node period. But on this time scale other, yet unexplained decade fluctuations, affect the earth's rotation rate.

11 Hydrology, Seismology and Volcanology

Hydrology offered the first historical observation of Earth Tides 2000 years ago.

Confined fluids indeed act as cubic strainmeters. Small cubic dilatations of the order of 10^{-8} induce easily observable water level tidal fluctuations of several centimetres in every well connected to confined fluid bodies.

As described by Strabon (Figure 1) these fluctuations are in opposition of phase with respect to the tidal potential: the low tide induces a compression which raises the liquid.

Even if such a natural instrument cannot be calibrated because we do not know the size and the porosity of the aquifer, this phenomenon is more than a pure curiosity because, comparing

⁴IRIS - International Radio Interferometric Surveying

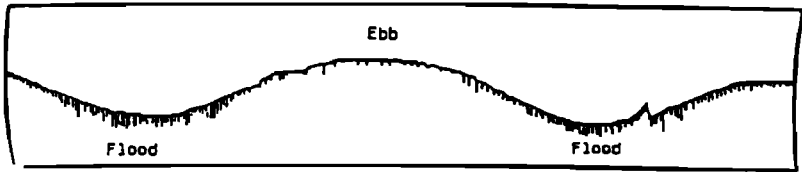


Figure 13: Level oscillations of the Tarka Bridge well (South Africa) showing gas-bubble effects.

the tidal response with the barometric efficiency of the well, it is possible to determine the storage coefficient of the formation and the volume porosity (Bredehoeft 1967).

As the porosity decreases with depth, the amplitude of the tidal fluctuations increases which is indeed observed in very deep wells.

Of course, not only common water wells are exhibiting tidal fluctuations but also oil wells, hydrothermal activity, geysers, volcanic lava and fumaroles, gas production, but direct observation is not easy in such cases. One may show, in this respect, the superposition of methane bubbles tidal release on the tidal fluctuations of the water level of a well at Tarka Bridge in South Africa (Figure 13).

The evidence of tidal strain and stresses effects in hydrology leads more and more authors to invoke tidal triggering as the cause of earthquake and volcanic activity. The strains are only of the order of 10^{-8} and consequently the stresses do not exceed 3 kilo Pascal. However, at tectonic time scales, this represents permanent very high frequency oscillatory stresses.

It is however difficult to explain that fortnightly periodicities are more often observed than diurnals or semi-diurnals ones.

On a world-wide basis the results appear somewhat inconclusive and, therefore, controversial, but when one restricts the search to a small region and one seismic crisis (for example an aftershock sequence), significant correlations have undoubtedly been noted.

As the amplitudes of the deformation and stress are highly dependent on the latitude and azimuth, it has been suggested that the orientation of the different components of the stress and strain tensors with respect to the fault planes orientations may be a sensitive factor (Souriau et al. 1982; Rydelek et al. 1988).

In the case of islands, the oceanic tidal loading may also play a more important effect than the direct Earth tide.

Volcanoes in Central America (Sadeh 1978), Pavlof (Alaska), Kilauea (Rydelek et al. 1988) Stromboli, Vesuvius and Etna (Johnston and Mauk 1972) are volcanoes where tidal effects have been identified in general for periods of 3 to 4 days before and after the eruption.

This tentative research of a tidal signal in earthquake swarms was certainly encouraged by the evident tidal signature observed in the periodicity of Moon quakes well related to the physical librations of the Moon.

Even a tidal signature was identified in geoelectric precursors of the Tangshan earthquake of 1976 (Fuye Qian et al. 1990).

The Bibliography on Earth Tides now contains not less than 92 papers devoted to these investigations, only 8 of them published prior to 1960.

*

* *

With the extraordinary increase of sensitivity of all geophysical or geodynamical equipments installed on or inside the earth's crust (broadband seismographs, superconducting gravimeters, strainmeters and tiltmeters, bottom pressure gauges) or embarked on board of our artificial satellites (laser retroreflectors, altimeter radars), a tidal signal appears in all measurements. We are thus confronted with two alternatives which can be efficiently handled by our powerful computers. Either we wish to eliminate this signal because it pollutes those other geophysical signals we are trying to analyze; and to do so, we need the most reliable model of combined tidal interactions. Or we want to use the different tidal responses of the Earth's complicate body to address new problems that the other geodynamic observations are not able to clarify like the mantle inelasticity, the core viscosity, the hydrodynamics of the core and the structure and role of boundary layers at the bottom and at the top of the liquid core.

Tidal researches which include the nutation phenomena offer us indeed new independent tools to go deeper in the Earth's structure and dynamics.

The subject is fascinating. It involves all these branches of Geophysics that our Union has, until now, successfully combined since 1919.

References

- [1] Beaumont, C., 1978. *Tidal loading: crustal structure of Nova Scotia and the M_2 tide in the northwest Atlantic from tilt and gravity observations.*
Geophys. J.R. Soc. 53, 27-53.
- [2] Beaumont, C. and Lambert, A., 1972. *Crustal Structure from Surface Load Tilts, Using a Finite Element Model.*
Geophys. J.R. Soc. 29, 203-226.
- [3] Cartwright, D.E. and Ray, R.D., 1989. *New Estimates of Oceanic Tidal Energy Dissipation from Satellite Altimetry.*
Geophys. Res. Letters, 16, nr 1, 73-76.
- [4] Cartwright, D.E. and Ray, R.D., 1990. *Oceanic Tides from Geosat Altimetry.*
J. Geoph. Res. 95, C3, 3069-3090.
- [5] Cartwright, D.E., Ray, R.D. and Sanchez, B.V., 1991. *Oceanic Tide Maps and Spherical Harmonic Coefficients from Geosat Altimetry.*
NASA Technical Memorandum 104544.
- [6] Cazenave, A. and Daillet, S., 1981. *Lunar Tidal Acceleration from Earth Satellite Orbit Analyses.*
J. Geoph. Res. 86, B3, 1659-1663.
- [7] Cazenave, A., 1982. *Tidal Friction Parameters from Satellite Observations.*
in "Tidal Friction and the Earth's Rotation II"
Springer-Verlag Berlin, 4-18.
- [8] Christodoulidis, D.C., Smith, D.E., Williamson, R.G. and Klosko, S.M., 1988. *Observed Tidal Braking in the Earth/Moon/Sun System.*
J. Geoph. Res. 93, B6, 6216-6236.

- [9] Dehant, V., 1987. *Integration of the gravitational motion equations for an elliptical uniformly rotating Earth with an inelastic mantle.*
Phys. Earth Planet. Int., 49, 242-258.
- [10] Dehant, V., 1987. *Tidal parameters for an inelastic Earth.*
Phys. Earth Planet. Int., 49, 97-116.
- [11] Dehant, V., Hinderer, J., Legros, M. and Leftitz, M., 1991. *Analytical computation of the long period Inner Core Wobble and of the Free Inner Core Nutations.*
IUGG General Assembly, Vienna, Union Symposium 6.
- [12] Dehant, V. and Zschau, J., 1989. *The effect of mantle inelasticity on tidal gravity: a comparison between the spherical and the elliptical Earth model.*
Geophys. Journal, 97, 549-555.
- [13] De Vries, D. and Wahr, J.M., 1991. *The Effects of the Solid Inner Core and Nonhydrostatic Structure on the Earth's Forced Nutations and Earth Tides.*
J. Geophys. Res. 96, B5, 8275-8293.
- [14] Felsentreger, T.L. and Marsh, J.G., 1979. *M₂ Ocean Tide Parameters and the Deceleration of the Moon's Mean Longitude from Satellite Orbit Data.*
J. Geophys. Res. 84, B9, 4675-4679.
- [15] Francis, O. and Mazzega, P., 1991. *What can we learn about Ocean Tides from Tide Gauge and Gravity Loading Measurements?*
11th Int. Symposium on Earth Tides, Helsinki, Schweizerbart'sche Verlagsbuchhandlung, Stuttgart, 287-298.
- [16] Gubanov, V. and Yagudin, L.I., 1978. *Earth tides according to the new USSR Standard Time system for 1955-1974.*
Sov. Astron. Lett 4, 57-59.
- [17] Hefty, J. and Capitaine, N., 1990. *The fortnightly and monthly zonal tides in the Earth's rotation from 1962 to 1988.*
J. Geoph. Int. 103, 219-231.
- [18] Hendershott, M.C., 1972. *The Effects of Solid Earth Deformation on Global Ocean Tides.*
J. Geoph. Res. 29, 389-402.
- [19] Herring, T.A., Gwinn, C.R. and Shapiro, I.I., 1986. *Geodesy by Radio Interferometry: Studies of the Forced Nutations of the Earth. I. Data Analysis; II. Interpretation.*
J. Geoph. Res. 91, B5, 4745-4754, 4755-4765.
- [20] Hough, S.S., 1895. *The oscillations of a rotating ellipsoidal containing fluid.*
Phil. Trans. Royal Soc. London, 186, 469-506.
- [21] Jeffreys, H., 1949, 1950. *Dynamic effects of a liquid core.*
Monthly Not. R. Astr. Soc., 109, nr 6, 670-687 and 110 nr 5, 460-466.

- [22] Jeffreys, H. and Vicente, R.O., 1957. *The theory of nutation and the variation of latitude*. Monthly Not. R. Astr. Soc., 117 nr 2, 142-161, 162-173.
- [23] Lambeck, K., 1975. *Effects of Tidal Dissipation in the Oceans on the Moon's Orbit and the Earth's Rotation*. J. Geoph. Res. 80, 20.
- [24] Lambeck, K., 1977. *Tidal dissipation in the oceans: astronomical, geophysical and oceanographic consequences*. Philos. Trans. R. Soc. London, A 287: 545-594.
- [25] Lambeck, K., Cazenave, A. and Balmino, G., 1974. *Solid Earth and Ocean Tides Estimated from Satellite Orbit Analyses*. Review of Geophysics and Space Physics, 12, 3.
- [26] Le Provost, Ch., Lyard, F. and Molines, J-M, 1991. *Improving Ocean Tide Prediction by Using Additional Semi-diurnal Constituents from Spline Interpolation in the Frequency Domain*. Geoph. Res. Letters, 18, 5, 845-848.
- [27] Love, A.E.H., 1909. *The yielding of the Earth to disturbing forces*. Proc. R. Soc. London, 82, 73-88.
- [28] Luo, S., Zheng, D., Robertson, D.S. and Carter, W.E., 1987. *Short-Period Variations in the Length of Day: Atmospheric Angular Momentum and Tidal Components*. Journal Geoph. Res., 92, B11, 11, 657-11, 661.
- [29] McNutt, S.R. and Beavan, R.J., 1984. *Patterns of Earthquakes and the effect of solid Earth and ocean load tides at Mount St. Helens prior to the May 18, 1980, Eruption*. Journal Geoph. Res., 89, B5, 3075-3086.
- [30] Marsh, J.G. and al., 1990. *The GEM-T2 Gravitational Model*. J. Geoph. Res., 95, B13, 22043-22071.
- [31] Matthews, P.M., Buffet, B.A., Herring, T.A. and Shapiro, I.I., 1991. *Forced Nutations of the Earth: Influence of Inner Core Dynamics. 1. Theory, 2. Numerical Results and Comparisons, 3. Very Long Interferometry Data Analysis*. J. Geophys. Res, 96, B5, 8219-8273.
- [32] Melchior, P., 1966. *Diurnal Tides and the Earth's Liquid Core*. Geoph. Journal Roy. Astr. Soc. 12, 15-21.
- [33] Melchior, P., 1971. *Precession-Nutations and Tidal Potential*. Celestial Mechanics 4, nr2, 190-212.
- [34] Melchior, P., 1980. *Luni solar Nutation Tables and the Liquid Core of the Earth*. Astronomy and Astrophysics 87, 365-368.

- [35] Melchior, P., 1982. *The Tides of the Planet Earth. 2nd Edition.*
Pergamon Press, 641 pages.
- [36] Melchior, P., and Georis, R., 1968. *Earth Tides, Precession-nutation and the Secular Retardation of Earth's Rotation.*
Phys. Earth Planet. Int., 14, 267-287.
- [37] Melchior, P. and De Becker, M., 1989. *A discussion of world-wide measurements of tidal gravity with respect to oceanic interactions, lithosphere heterogeneities, Earth's flattening and inertial forces.*
Physics of the Earth Planet. Interiors, 31, 27-53.
- [38] Merriam, J.B., 1985. *Lageos and UT Measurements of Long-Period Earth Tides and Mantle Q.*
J. Geoph. Res., 90, B11, 9423-9430.
- [39] Miller, G.R., 1966. *The flux of tidal energy out of the deep oceans.*
Journ. Geophys. Res. 71, 2485-2489.
- [40] Molodenskii, M.S., 1961. *The Theory of Nutations and Diurnal Earth Tides.*
IVe Symp. Int. sur les Marées Terrestres. Obs. Roy. Belg. Comm. nr 188, S. Geoph. 58, 25-56.
- [41] Morrison, L.V. and Ward, C.G., 1975. *An Analysis of the Transits of Mercury: 1677-1973.*
Mon. Not. R. Astr. Soc., 173, 183-206.
- [42] Neuberg, J., Hinderer, J. and Zürn, W., 1987. *Stacking gravity tide observations in central Europe for the retrieval of the complex eigenfrequency of the nearly diurnal free-wobble.*
Geoph. J. Roy. Astr. Soc. 91, 853-868.
- [43] Parke, M.E., 1982. *O1, P1, N2 Models of the Global Ocean Tide on an Elastic Earth Plus Surface Potential and Spherical Harmonic Decompositions for M2, S2 and K1.*
Marine Geodesy, 6, nr 1, 35-81.
- [44] Parke, M.E. and Hendershott, M.C., 1980. *M2, S2, K1 Models of the Global Ocean Tide on an Elastic Earth.*
Marine Geodesy, 3, 379-408.
- [45] Platzman, G.W., 1984. *Planetary Energy Balance for Tidal Dissipation.*
Rev. Geophys. Space Physics. 22, nr 1, 73-84.
- [46] Platzman, G.W., 1985. *The Role of the Earth Tides in the Balance of Tidal Energy.*
J. Geoph. Res. 90, nr B2, 1789-7893.
- [47] Poincaré, H., 1910. *Sur la précession des corps déformables.*
Bull. Astron. 27, 321-356.

- [48] Rydelek, P.A., Davis, P.M. and Koyanagi, R.Y. 1988. *Tidal triggering of earthquake swarms at Kilauea Volcano, Hawaii*.
Journ. Geoph. Res. 93, B5, 4401-4411.
- [49] Schwiderski, E.W., 1980. *On Charting Global Ocean Tides*.
Review of Geoph. and Space Phys., 18, 1, 243-268.
- [50] Schwiderski, E.W., 1980. *Ocean Tides, Part I: Global Ocean Tidal Equations*.
Marine Geodesy, 3, 161-217.
- [51] Schwiderski, E.W., 1980. *Ocean Tides, Part II: A Hydrodynamical Interpolation Model*.
Marine Geodesy, 3, 219-255.
- [52] Schwiderski, E. W., 1983. *Atlas of Ocean Tidal Charts and Maps, Part I: The Semi-diurnal Principal Lunar Tide M₂*.
Marine Geodesy, 6, 3-4, 219-265.
- [53] Schwiderski, E.W., 1985. *On Tidal Friction and the Decelerations of the Earth's Rotation and Moon's Revolution*.
Marine Geodesy, 9, 4, 399-450.
- [54] Sloudsky, Th., 1895. *De la rotation de la Terre supposée fluide à son intérieur*.
Bull. Soc. Imp. Nat. Moscou IX, 285-318.
- [55] Smith, M.L., 1977. *Wobble and nutation of the Earth*.
Geophys. J. Roy. Astr. Soc., 50, 103-140.
- [56] Souriau, M., Souriau, A. and Gagnepain, J., 1982. *Modeling and Detecting Interactions between Earth Tides and Earthquakes with Application to an Aftershock Sequence in the Pyrénées*.
Bull. Seismological Soc. Amer. 72, nr 1, 165-180.
- [57] Thomas, J.P. and Woodworth, Ph. L., 1990. *The Influence of Ocean Tide Model Corrections on Geosat Mesoscale Variability Maps of the North East Atlantic*.
Geoph. Res. Letter, 17, 12, 2389-2392.
- [58] Wahr, J.M., 1981. *A normal mode expansion for the forced response of a rotating Earth*.
Geoph. J. Roy. Astron. Soc., 64, 3, 651-676.
- [59] Wahr, J.M., 1981. *Body tides on an elliptical, rotating, elastic and oceanless Earth*.
Geoph. J. Roy. Astron. Soc., 64, 3, 677-704.
- [60] Wahr, J.M., 1981. *The forced nutations of an elliptical, rotating, elastic and oceanless Earth*.
Geoph. J. Roy. Astron. Soc., 64, 3, 705-728.
- [61] Wahr, J.M., Sasao, T. and Smith, M.L., 1981. *Effect of the fluid core on changes in the length of day due to long period tides*.
Geoph. J. Roy. Astron. Soc., 64, 3, 635-650.

- [62] Wahr, J. L. and Sasao, T., 1981. *A diurnal resonance in the ocean tide and in the Earth's load response due to the resonant free core nutation.*
Geoph. J. Roy. Astron. Soc., 64, 3, 747-765.
- [63] Wahr, J. L. and Bergen, Z., 1986. *The effects of mantle anelasticity on nutations, Earth tides, and tidal variations in rotation rate.*
Geophys. J. R. Astr. Soc. 87, 633-668.
- [64] Williams, E., 1990. *Tidal Rhythmites: Key to the History of the Earth's Rotation and the Lunar Orbit.*
J. Phys. Earth, 38, 475-491.
- [65] Woodworth, P. L., 1985. *Accuracy of existing ocean tide models.*
Proceedings of a Conference on the Use of Satellite Data in Climate Models, Alpbach, Austria, 95-98.
- [66] Zhu, S. Y. and Groten, E., 1989. *Various Aspects of Numerical Determination of Nutation Constants. I. Improvement of Rigid-Earth Nutation.*
Astron. J. 98, 3, 1104-1111.
- [67] Zschau, J., 1986. *Tidal Friction in the Solid Earth: Constraints from the Chandler Wobble Period.*
Space Geodesy and Geodynamics, Academic Press Inc. London, 315-344.

N.B. For a more complete list of references see Melchior, 1982.